SC-4144(TR)
TID-4500 (15th Ed.)
HEALTH AND SAFETY

A STUDY OF NEVADA TEST SITE WIND VARIABILITY

Jack W. Reed

March 1958

Reprinted July 1, 1960

Sandia Corporation
CONTRACTORS FOR U.S. ATOMIC ENERGY COMMISSION
ALBUQUERQUE • NEW MEXICO

Published by Sandia Corporation,
a prime contractor to the
United States Atomic Energy Commission

Printed in USA. Price $1.50. Available from the Office of
Technical Services, Department of Commerce,
Washington 25, D. C.

SC-4144(TR)
TID-4500 (15th Ed.)
HEALTH AND SAFETY

A STUDY OF NEVADA TEST SITE WIND VARIABILITY

Jack W. Reed

March 1958

Reprinted July 1, 1960

ABSTRACT

Wind observations collected at Yucca Flat since 1951 are analyzed for timewise variability. Variability functions of altitude, season, wind speed, and vector wind are described. Derived variability parameters are incorporated into calculations of fallout safety probability for NTS operations.

TABLE OF CONTENTS

	Page
ABSTRACT	1
Introduction	7
Data Reduction	8
Winds-Aloft Climatology	9
Winds-Aloft Changes with Time, Season, and Altitude	10
Wind Change Relations to Synoptic Weather Patterns	13
Wind Forecast Evaluation	14
Fallout Safety Probability Computations	17
Summary	20
Additional Notes	21
APPENDIX A	45
LIST OF REFERENCES	51

LIST OF ILLUSTRATIONS

	Page
Fig. 1 -- Standard vector deviation wind rose, Las Vegas (summer)	23
Fig. 2 -- Standard vector deviation wind rose, Las Vegas (winter)	25
Fig. 3 -- Spring wind variability	27
Fig. 4 -- Summer wind variability	28
Fig. 5 -- Fall wind variability	29
Fig. 6 -- Winter wind variability	30
Fig. 7 -- Wind variability comparisons	31
Fig. 8 -- Time variability versus altitude relation (spring)	31
Fig. 9 -- Annual march of wind variability	32
Fig. 10 -- Wind change versus altitude relation (spring)	33
Fig. 11 -- Interpolation chart for wind variability (spring)	34
Fig. 12 -- Wind speed versus variability (spring)	35
Fig. 13 -- Mercury 24-hour vector standard deviation for 30,000-foot-MSL wind vectors (spring)	36
Fig. 14 -- Mercury 24-hour vector variability for 30,000-foot-MSL wind vectors (summer)	37
Fig. 15 -- UPSHOT-KNOTHOLE wind forecast errors	38
Fig. 16 -- TEAPOT wind forecast errors	39
Fig. 17 -- Component error distributions, 1953 (12-hr)	40
Fig. 18 -- Wind component error distribution (24-hr)	40
Fig. 19 -- Mercury 24-hour vector variability proportion of standard 32.1-knot deviation for 30,000-foot-MSL wind vectors (spring)	41
Fig. 20 -- Fallout safety probability computation chart	43

LIST OF TABLES

	Page
TABLE I -- Wind Change Standard Deviation	11
TABLE II -- Wind Forecast Errors	15
TABLE III -- Vector Standard Errors	17
TABLE IV -- Seasonal Coefficients of Variability	18
TABLE V -- Hours From Wind Observation Until Time Particle Lands at 4000 MSL, ΔT, and Trajectory Standard Vector Error, σ	19
TABLE A-I -- Table for Resolving Polar Coordinate Wind Observations to X (west-east) and Y (south-north) Component Winds (W_x, W_y)	47
TABLE A-II -- Wind Resolution to X (west-east) and Y (south-north) Components (W_x, W_y)	49
TABLE A-III -- Component Squares (W_x^2, W_y^2)	49
TABLE A-IV -- Covariances (W_x, W_y)	49

A STUDY OF NEVADA TEST SITE WIND VARIABILITY

Introduction

Calculation of fallout safety probability (Ref 1) requires a knowledge of wind variability. This quantity appears, in turn, to be influenced by several other factors: possibly season, altitude, synoptic weather type, wind speed and, of course, geographical location. Fortunately, some early surveys (Refs 2 and 3) of wind variability were made near the Nevada Test Site (NTS) and at Muroc and Salton Sea, California. In general, their results should be representative for application to atomic test problems. However, effects of the other factors were not extensively evaluated.

To gain a more precise estimate of safety probabilities for each specific atomic test, a further breakdown of data—beyond year-round types of averages—was requested by the Test Advisory Panel Chairman, Dr. A. C. Graves. Since forecasting capability may also be used in computing safety probability, an analysis of past performance in wind forecasting by the Air Weather Service (AWS) forecasting center was deemed necessary by the Meteorology Subcommittee of the NTS Planning Board. It was hoped that on the eve of a test an objective statement of wind variability could be produced which would include the effects of the various factors mentioned above, together with an influence from the forecaster's 'feeling' of confidence in the forecast presented. This feeling comes from experience in recognizing that, although some weather patterns move or change rapidly, others remain fairly stable. During TEAPOT and earlier test operations, the Advisory Panel had to make shot decisions from only subjective estimates of the situation, with obviously restricted efficiency.

Finally, computer charts for estimating fallout safety probability are required; these are made from weather data observed at NTS and incorporate additional variables of consequence in assessing wind variability and fallout particle trajectory uncertainty.

Statistical analyses in this report were derived from observations of winds aloft made by the AWS at Yucca Flat during various periods since early 1951. Original weather records are stored in the National Weather Records Center, Asheville, North Carolina. Microfilm copies were furnished to Sandia Corporation by the Special Projects Section, United States Weather Bureau. Collections of wind forecasts, prepared by the AWS during UPSHOT-KNOTHOLE (UK) and TEAPOT operation periods, were furnished by the FC/AFSWP, Weapons Effects Test Directorate Staff Weather Officer. Data reduction assistance was provided by Sandia Corporation Test Data Department, 5240.

Data Reduction

Both winds-aloft forecasts and observations give wind direction (degrees) and wind speed (knots) at specified mean sea level (MSL) altitudes. In this study, data from the 5000-, 10,000-, 15,000-, ..., and 50,000-foot levels were used.

Since wind speeds and directions and their changes are not unrestricted variables (ie, wind speed cannot be less than zero and a direction change of more than 180 degrees would not be recorded), the most meaningful wind statistics are obtained from wind-component (x, y) tabulations. Then normal distribution-curve parameters may be employed for comparisons rather than more complex distribution functions which are necessary for interpreting polar coordinate data. To facilitate conversion of polar coordinate data to Cartesian coordinate data, a table constructed (Appendix A) for speeds up to 120 knots shows x- (positive for wind blowing toward east) and y- (positive for wind blowing toward north) component winds to the nearest knot for each wind direction. (Wind directions are forecast and observed only to the nearest 10 degrees).

When all observations had been tabulated in component form, timewise component changes were computed. To obtain the component change for each time interval, each observation was compared with the observation made at the same height level 3, 6, 12, and 24 hours previously. In normal practice, wind-balloon runs are made at regular 6-hour intervals, at 0300, 0900, 1500, and 2100Z* (Greenwich Mean Time). However, NTS requirements often called for extra observations, and a normal observation schedule was not usually kept. Therefore, in this study, wind changes over the time intervals 2-4, 5-7, 10-14, and 20-28 hours were accepted as 3-, 6-, 12-, and 24-hour changes, respectively. It is felt that errors introduced by this range of time intervals are much smaller than might have been experienced through a sizable reduction of the data sample size.

Tabulations of forecasts were similarly compared with observations made at forecast verification times. A separate tabulation of wind changes during each forecast period was also made for comparison of forecast errors to observed shifts.

Since forecasts were prepared only when conditions (weather and/or technical) were at least partly favorable for tests, this selectivity might have biased the sample distribution from the seasonal normal, and, since no formal statement of the forecaster's confidence in a specific prediction was furnished, no relative weighting of forecasts under different conditions was possible. Such statements of high or low confidence were made during briefings associated

*World-wide upper air observing times were changed to 0000, 0600, 1200, and 1800Z in June 1957.

with some of these forecasts but were not recorded. A more objective, or at least enumerable, statement would be required before a valid weighting procedure could be employed in the verification.

As a further point in data reduction, when abnormally large wind shifts were recorded from coded observation data, the microfilm record was checked to see whether an obvious error in reporting had been made. In many instances, a mistake was found easily but, without recomputation of the balloon run, other large shifts had to be accepted. However, this type of error would also be present in raw observations fed into any effects calculations made in the field; therefore, it may be regarded simply as an insignificant portion of total instrument error, which, of course, contains round-off components of real significance when 10-degree angular resolution is employed. Instrument error in wind-observing systems is very difficult to assess (Ref 4), but is small compared to time shifts for time scales considered in this study; therefore, it has been ignored completely.

Winds-Aloft Climatology

Average winds and distributions could be obtained from NTS observations but, since most of the data were observed during the spring season, other season averages might be biased by small sample size, as might any over-all averages. Consequently, published winds-aloft distributions for Las Vegas, Nevada (Ref 5), were used to construct vector-distribution wind roses (Ref 6). These data are likely to be more representative of NTS conditions than the smaller number of observations actually made at Yucca Flat. Six wind roses of this type are shown (Figs. 1 and 2) for summer and winter seasons and at the 700-, 300-, and 200-millibar constant pressure surfaces. These surfaces occur at about 10,000-, 30,000-, and 40,000-foot-MSL altitudes, respectively. The isoprobability ellipses contain 50 percent ($0.83\vec{\sigma}$) and 90 percent ($1.52\vec{\sigma}$) of the observations, respectively.

Since wind frequency distribution tables (Ref 5) are usually made with 16-point compass-heading wind directions with speed intervals of 10 knots, a set of tables for conversion to wind components, component squares, and component products—needed in constructing vector-distribution wind roses—is furnished in Appendix A. A summation of table values multiplied by relative occurrence frequencies in corresponding range blocks of wind-distribution tables gives wind-component means, variances, and covariances.

The structure of these roses is of no direct significance in fallout safety estimation except that it is useful to have a general feeling for the parent population of winds when considering wind change statistics. With some assumptions and a knowledge of the character of timewise wind correlation coefficients, timewise wind change statistics could be derived from distribution roses; however, a direct observation of change statistics is provided in this report.

Winds-Aloft Changes With Time, Season, and Altitude

A table showing standard deviations of vector wind changes for each component direction and the total vector for each season and altitude and for 3-, 6-, 12-, and 24-hour periods was needed. Lack of sufficient observations precluded complete results, but most of the requirements were met. Hand computation was done for all statistics, as the data sample was considered too small and inhomogeneous for electronic data processing. Electronic calculation programming would have taken nearly as many man-hours as were required for hand computation.

To make it easier to reduce the data by hand, the vector component standard deviations have been estimated from the sample mean deviation rather than from the sample standard deviation. If the distribution of component changes is normal with mean zero and variance (σ^2), the average value of the sample mean deviation is

$$|\bar{x}| = \sqrt{\frac{2}{\pi}}\,\sigma \int_0^{+\infty} e^{\frac{x^2}{2\sigma^2}}\, x\,dx = \sqrt{\frac{2}{\pi}}\,\sigma\,, \tag{1}$$

and thus

$$\sigma \approx 1.254\ |\bar{x}|\ . \tag{2}$$

It will be shown later that wind changes are not exactly normally distributed, since a slightly abnormal number of large changes are observed. This causes standard deviations (σ), calculated from average deviations, to be slightly smaller than standard deviations obtained from sums of squares of deviations. Numerical checks of sigmas calculated from observed data verified this condition but, in general, no large discrepancies were noted, so abnormalities in the distribution have been disregarded.

Standard deviations estimated from sample means of wind changes by components and for total change vectors are shown (Table 1) for various seasons, altitudes, and observing intervals, as well as the number of observations available for computing each standard deviation. Data from Table 1 are presented graphically in Figs. 3 through 6. Each figure in this set presents, for a season and observing interval, a curve of standard deviation versus altitude. Short dashes are used for the west-east (x) component wind changes, long dashes for the south-north (y) component changes, and a solid line for the magnitude of the vector standard changes. In nearly every instance, south-north component changes are larger than west-east component changes. This may be broadly interpreted, for westerly mean winds, as indicating a predominance of wind-direction changes over wind-speed changes.

TABLE I

Wind Change Standard Deviation
(knots)

Altitude (kft)	Component	Spring				Summer			Fall		Winter		
		Time interval (hr)				Time interval (hr)			Time interval (hr)		Time interval (hr)		
		3	6	12	24	6	12	24	12	24	6	12	24
5	x	5.2	6.7	7.7	7.4	5.7	6.1	5.7	7.2	6.0	4.8	5.3	5.7
	y	7.4	9.2	12.4	13.5	8.9	11.8	8.5	8.2	7.0	9.3	9.9	10.5
	→	9.0	11.4	14.6	15.4	10.6	13.2	10.1	10.9	9.2	10.4	11.2	11.9
	n	168	763	807	943	45	41	92	91	96	20	146	195
10	x	6.9	7.7	9.5	11.1	7.8	7.9	7.8	8.1	10.2	8.3	13.4	15.2
	y	7.2	9.4	12.2	15.5	8.8	9.8	9.5	9.4	12.0	10.8	16.1	21.7
	→	10.0	12.2	15.5	19.1	11.8	12.6	12.3	12.4	15.8	13.6	21.0	26.5
	n	167	772	807	944	45	41	92	93	98	20	148	197
15	x	6.9	9.5	12.4	15.5	9.6	9.6	11.3	8.9	11.4	14.7	16.5	20.2
	y	8.3	11.8	14.7	19.9	9.1	15.0	15.7	11.7	15.6	16.0	17.6	23.1
	→	10.8	15.2	19.2	25.2	13.2	17.8	19.1	14.7	19.3	21.8	24.1	30.7
	n	169	774	803	943	45	41	92	93	99	19	145	191
20	x	9.6	12.5	15.1	21.0	9.0	9.0	11.9	10.3	12.8	16.8	18.7	24.1
	y	9.2	13.4	18.5	26.2	11.4	11.2	17.0	14.4	19.8	17.5	23.6	31.5
	→	13.3	18.4	23.9	33.5	14.5	14.4	20.4	17.7	23.6	24.2	30.1	39.7
	n	168	756	779	918	45	41	90	91	95	13	141	174
25	x	11.6	14.0	17.9	24.3	10.2	10.0	16.2	12.5	17.7	18.2	24.2	31.5
	y	11.9	15.7	22.6	31.8	14.0	11.0	22.0	16.0	22.3	21.0	29.6	39.6
	→	16.6	21.1	28.8	40.0	17.4	14.9	27.0	20.4	28.5	27.8	38.2	50.6
	n	164	734	756	894	44	38	87	79	86	4	141	142
30	x	11.8	16.3	21.2	28.1	12.0	12.1	18.4	17.4	21.3		26.4	32.8
	y	12.4	18.3	25.4	35.8	18.9	16.6	27.7	17.5	22.9		31.6	45.5
	→	17.1	24.4	33.1	45.5	22.5	20.6	31.5	24.7	31.2		41.2	56.1
	n	153	702	723	853	42	36	81	75	83		124	129
35	x	13.9	16.9	21.5	28.4	15.6	18.7	26.1	19.6	24.3		26.0	33.3
	y	12.4	18.2	26.3	36.4	17.9	20.0	29.7	24.3	28.2		30.4	44.4
	→	18.6	24.9	34.0	46.2	23.7	27.4	39.5	31.2	37.2		40.1	55.5
	n	142	650	668	789	38	32	75	68	77		97	96
40	x	16.2	16.8	20.5	26.1	11.1	13.4	21.5	17.2	21.9		29.1	34.8
	y	12.8	17.8	24.4	32.2	20.6	18.4	24.7	17.7	21.7		32.0	37.9
	→	20.6	24.4	31.9	41.4	23.4	22.7	32.7	24.7	30.9		43.2	51.5
	n	134	562	576	700	34	27	64	58	64		78	80
45	x	13.9	16.6	16.9	21.8	10.7	9.1	18.7	13.4	19.3		26.6	27.0
	y	10.6	15.3	19.3	27.0	16.0	12.4	15.8	15.1	20.9		31.1	34.7
	→	17.4	22.5	25.6	34.7	19.2	15.4	24.4	20.2	28.5		40.9	44.1
	n	112	424	412	538	25	21	49	45	50		53	60
50	x	12.3	14.2	16.4	19.0	14.8	10.6	10.1	11.9	12.2		24.5	32.0
	y	9.9	13.3	15.7	20.8	17.6	9.6	9.2	14.7	16.8		24.9	29.0
	→	15.8	19.4	22.7	28.2	23.0	14.2	13.6	19.0	20.8		35.0	43.3
	n	82	310	302	410	12	13	32	26	28		38	43
All levels (vector)		15.1	19.2	25.5	32.1	18.6	17.9	25.0	20.4	25.8	20.6	34.0	43.2

A very interesting feature of the observed variability for nearly every time interval is the marked peak at 35,000 feet. This was not noticed in studies of short-time-interval variability (Refs 2 and 3). The drop above the peak also went unnoticed in other studies which did not have adequate data at higher altitudes. Preliminary studies of Eniwetok wind data show that variability appears to decrease to a minimum in the high stratosphere near 100,000 feet, which is also near the upper altitude limit of current balloon-sounding techniques.

The all-level weighted standard deviation of change from Table I is plotted against time interval for each season in Fig. 7 and compared to time-interval variability data from other

referenced sources. Data collected by Reed (Ref 2) for 1-hour time intervals over a January-to-July period at Salton Sea Test Base, California, for all altitudes to 40,000 feet MSL lumped together, showed a variability of 3.7 knots. On individual days of the sample, variability ranged from 2.2 to 5.2 knots. In the same geographical region, Singer (Ref 3) obtained data at Edwards Air Force Base, Muroc, California, over several time intervals and at altitudes ranging from 3000 to 38,000 feet MSL. Variabilities averaged from 2.0 knots at 1/2-hour intervals to 6.6 knots at 5-hour intervals. From observations made at Fort Monmouth, New Jersey, at altitudes to 20,000 feet MSL, Arnold (Ref 7) reported variabilities of 0.97 knot at 1/2-minute intervals, 1.2 knots at 5-minute intervals, and 4.2 knots at 90-minute intervals. A British report (Ref 8) gave variabilities for levels to 15,000 feet MSL, ranging from 3.3 knots at 1/2-hour intervals to 7.1 knots at 6-hour intervals. Finally, data obtained from Project Rawijet (Ref 9) at Salton Sea showed that variability was greater with jet streams in the neighborhood. Three days' data (Ref 4), to 50,000 feet MSL, yielded variabilities of 5.9 knots at 1-hour intervals and 17 knots at 6-hour intervals.

NTS data appear to show greater variabilities than other sources, but this is most probably due to use of more high altitude data in the region of the tropopause and jet streams. It agrees fairly well with Rawijet data from Salton Sea. Thin reference lines are shown for approximating variability proportionally to the square root of time interval. Several of the data groups appear to parallel these lines and verify the relation $\sigma = kT^{1/2}$, previously reported (Ref 2).

Another plot of time variability for various altitudes, using spring NTS data from Table I, is shown in Fig. 8. Again, the separate altitude curves generally agree with the $T^{1/2}$ slope. The major deviations are for high and low altitudes, and can be explained. At high altitudes, instrument errors are relatively large and affect short-time-interval wind changes relatively more than long-time-interval changes. At low altitudes, where wind speeds are low, variability is consequently more restricted than at high altitudes, a restriction which affects long-time intervals most strongly. For example, if we assume maximum speed to be 100 knots and direction difference to be 180 degrees, the maximum wind change in a near infinite time (since weather observation began) would be about 200 knots at the surface, but it might be over 500 knots at jet-stream level. These influences cause the slope of the $\sigma(T)$ curves at low and high altitudes to be less than the slope for other altitudes.

Seasonal influences on variability are illustrated in Fig. 9, where the summer minima and winter maxima are seen reflected at all altitude levels. At low levels, seasonal oscillation amplitude is reduced because strong convective turbulence experienced in summer gives about the same effect as synoptic-scale flow pattern changes occurring with frequent frontal passages in winter.

A graph of springtime vector variability versus altitude, with curves for 3-, 6-, 12-, and 24-hour time intervals, is shown in Fig. 10. Using $T^{1/2}$ time dependence, curves were fitted by the method of least squares by weighting each point by the number of data values it represents. Neither the cubic nor quartic approximation appears to make a very close fit to the data, but they will be used to greatly simplify trajectory error calculations. Actually, for 12-hour intervals and less, and below 40,000 feet, the quartic approximation is seemingly adequate. The fitting equations derived are:

$$\vec{\sigma} = (\text{T hours})^{1/2} (1.234 + 0.2801h + 0.003681h^2 - 0.0001332h^3) \text{ knots}, \quad (3)$$

and

$$\vec{\sigma} = (\text{T hours})^{1/2} (0.1831 + 0.5851h - 0.01111h^2 + 0.00003326h^3 + 0.0000003290h^4) \text{ knots}. \quad (4)$$

In each equation, h is altitude in thousands of feet (kilofeet) MSL. Adequate data were not available for a similar calculation for other seasons.

Logarithmic interpolation curves (Fig. 11) are furnished for calculating trajectory error from data rather than from a fitted equation. Also, curves drawn from a $T^{0.366}$ relationship, which fits spring data (Fig. 7), are shown for extrapolation down to 1/2-hour intervals.

Wind Change Relations to Synoptic Weather Patterns

Wind variability may be expected to vary with types of general atmospheric circulation patterns. With a regime of high-amplitude pressure waves moving rapidly from west to east, winds at any point should show much greater changes than when a pattern of low-amplitude waves is moving slowly. To furnish prediction analogues, many attempts have been made in past years to 'type' weather patterns by some logical system. Such attempts have not met with notable success, but various agencies are still trying, particularly with electronic brain catalogue programs. However, it appears that no simple, yet accurate, method for analogue typing will ever be found. Thus, no attempt has been made to relate observed wind shifts with what is called synoptic pattern, or type.

However, correlations may be expected between variability and either wind speed or wind vector, since these are a product of the weather pattern. Singer (Ref 3) has shown that variability increases with wind speed to the extent that either 1-hour or 5-hour changes are doubled as initial speed is increased from calm to 50 mph. Salton Sea data (Fig. 7) also show high variability associated with observation of high-speed jet streams.

To check this dependence with NTS data, another data tabulation was made of standard deviations of vector wind changes taken over all altitudes for each observed balloon run. This variability expression was tabulated against the observed initial 30,000-foot-MSL wind vector.

This altitude was selected as being nearest any jet-stream core, since jet-stream parameters are currently considered to be strong influencing factors in general weather forecasting.

Scatter diagrams of variability versus wind speed were constructed from tabulated 1955 springtime data for 3-, 6-, 12-, and 24-hour intervals (Fig. 12). From data for 6-hour shifts (Fig. 12b), a linear regression line was computed to show

$$\vec{\sigma} = 3.42 + 0.25|\overrightarrow{W_o}| \text{ knots.} \quad (5)$$

The standard error in using this estimate would be ±8.2 knots. Thus, no close correlation of wind variability with wind speed, disregarding direction, obtains.

When 24-hour variability was plotted for wind vectors on polar coordinate charts, a pattern was recognized. Severe smoothing was necessary to give a pattern simple enough to be useful, as shown in Fig. 13. This smoothing was done first by averaging variability over 20-degree direction and 20-knot speed intervals. Contour lines were lightly drawn to fit the numbers as shown. The heavy contour pattern was then drawn, smoothing by eye, to give a simple representation of the variability-wind vector relationship. The heavy solid contour portions are made through regions where ten or more observations of variability were available for averaging. Dashed lines represent four to nine points used in averaging. Dotted portions are uncertain estimates based on less than four observations.

The most striking feature of the pattern is noted by comparison with Figs. 1b and 2b, which show distributions of wind vectors for summer and winter. Whereas the most frequently observed springtime winds are moderate west-southwesterlies, the most stable flows are light-to-moderate north-northwesterlies. It is also clearly shown that rare occurrences of south-through-east winds are most variable.

A similar chart was constructed for summertime 24-hour variability (Fig. 14). This time, the stability pattern is aligned with the occurrence pattern of Fig. 1a. So, in summer, prevailing moderate-speed southwesterlies also represent the most durable patterns.

Data for analysis of other seasons' variability were limited, as they were for summer. Consequently, it was felt that the derived springtime pattern could be used for fall and winter almost as reliably as an analysis based on only 100 observations. Furthermore, a seasonal separation should be made by climatological season rather than calendar season for proper homogeneity of data (Ref 10). When more NTS data have been collected, this refined breakdown can be made.

Wind Forecast Evaluation

Standard errors of wind forecasts made during 1953 and 1955 test periods are shown in Table II. These 12-hour and 24-hour forecasts were delivered 12 and 24 hours before verification time. Thus, the forecasts were made from still earlier observations. Results are

shown as vector errors broken down by operation, forecast period, altitude, and direction component. Vector errors which would have been made in assuming persistence during the same forecast intervals are shown for comparison. Data from Table II are depicted in Fig. 15a for UK 12-hour forecasts; in Fig. 15b for UK 24-hour forecasts; in Fig. 16a for TEAPOT 12-hour forecasts; and in Fig. 16b for TEAPOT 24-hour forecasts. Small data samples caused ragged curves and do not allow point-by-point comparisons with persistence. However, vector standard deviations for all data from all levels are also shown in Table II for a general comparison of the forecast system. Note that all UK 12-hour forecasts had a standard vector error of 34.9 knots, while persistence would have erred only by 27.6 knots. Thus, forecasts were 26 percent worse than persistence. Similarly, UK 24-hour forecasts were 19 percent better than persistence; TEAPOT 12-hour forecasts were 8 percent better than persistence; and TEAPOT 24-hour forecasts were 2.3 percent better than persistence.

TABLE II

Wind Forecast Errors

Altitude (kft)	UPSHOT-KNOTHOLE Forecast errors σ_x	σ_y	$\vec{\sigma}$	Change $\vec{\sigma}$	n	TEAPOT Forecast errors σ_x	σ_y	$\vec{\sigma}$	Change $\vec{\sigma}$	n
12-hour forecast errors (knots)										
5	3.7	8.1	8.9	15.3	19	4.8	8.2	9.5	11.0	14
10	12.9	10.1	16.4	15.3	19	9.6	14.7	17.5	15.2	14
15	11.5	14.7	18.7	20.5	16	9.5	11.2	14.6	17.5	14
20	11.7	15.6	19.5	24.4	19	16.7	13.8	21.7	30.0	14
25	21.0	16.5	26.7	25.7	16	16.1	17.4	23.7	31.7	14
30	23.0	31.1	38.7	33.4	17	15.4	15.7	22.0	39.3	14
35	27.2	44.5	52.2	42.7	13	21.5	19.1	28.8	39.2	14
40	32.3	35.9	48.3	42.5	15	14.9	20.5	25.3	28.3	14
45	57.1	22.1	61.2	18.4	5	13.4	22.9	26.6	21.6	14
50	25.3	26.2	36.4	20.9	2	15.3	13.0	20.1	17.7	13
All levels			34.9	27.6	141			21.7	26.9	139
24-hour forecast errors (knots)										
5	3.3	8.5	9.1	9.9	13	5.6	9.6	11.1	14.4	22
10	14.2	20.4	24.9	18.9	14	13.5	15.0	20.2	18.9	22
15						15.2	16.7	22.6	29.8	22
20	20.2	27.6	34.2	38.6	14	20.1	18.9	27.5	31.0	22
25						22.9	23.4	32.7	34.4	22
30	29.1	43.3	52.1	62.6	13	31.4	24.0	39.5	41.7	22
35						31.1	29.9	43.1	39.4	22
40	40.3	46.1	61.2	59.7	11	23.4	27.0	35.7	33.9	22
45						18.0	21.2	27.8	29.6	22
50						15.6	15.9	22.3	24.7	12
All levels			39.8	42.2	65			30.0	30.7	210

Two conclusions may be drawn from the results. First, no great gain is obtained by using forecast winds rather than assuming persistence of latest observations. Second, the error-versus-altitude pattern for forecasts is similar to the pattern for persistence error (or wind variability). It follows that more changeable conditions at higher altitudes are more difficult to forecast than less changeable conditions at lower altitudes. It may well be assumed, therefore, that this direct relation between forecast capability and wind changeability holds also for changes of season, geography, etc.

Component error distributions from 1953 12-hour forecasts and their associated wind shifts are tabulated and graphed in probability coordinates (Fig. 17). These curves show that over 80 percent of each data sample is approximately normally distributed. Straight lines nearly follow the data points from 10 percent to 90 percent of each sample. In the large error regions, data show that forecasts have an abnormal tendency to greatly overestimate both southerly and westerly wind components. This is compared to a tendency toward a slightly abnormal number of large west wind decreases and an abnormal number of large south wind increases. However, this data sample is much too small to give reasonable confidence in any extreme value analysis.

The main point to be stressed from this distribution analysis is that, for the most part, forecast errors are the same as errors which would have been made in assuming persistence over a forecast period. Also, the demonstrated normal distribution of errors and shifts alike allows ordinary probability treatment of resulting effects.

Analysis of 24-hour forecast error and change distribution was made without regard for algebraic sign of errors. If it is assumed that the distribution is symmetric about zero, this procedure has the effect of doubling the data in smoothing the appearance of the distribution. Distribution curves of component error and change are shown (Fig. 18) for 24-hour forecasts made during both operations, UPSHOT-KNOTHOLE and TEAPOT. Either plus or minus signs may be ascribed to the component error coordinate. Again, it is evident that forecast errors are nearly equal to and distributed similarly to wind changes over like periods. This diagram also shows that the apparently superior capability (Table II) of the TEAPOT weather section over the UK group is mainly due to smaller variability in TEAPOT winds. Another point of note is that the less variable TEAPOT data more nearly fit a normal distribution. It appears that most small changes of wind are caused by random turbulent cells, but large shifts occur more frequently than turbulence theory would indicate. This additional occurrence of large changes is no doubt associated with fronts, waves, and discontinuous flow features which meteorologists attempt to predict.

The argument is always made, when discussing forecast capability, that the forecaster may not accomplish anything on the average, but this is due to a few large misses under especially difficult situations. It is further claimed that a good forecaster can recognize, in

advance, his low- and high-confidence forecasts. Data used in this analysis do not include confidence ratings, but, instead, a confidence factor—based on the functional relationship between wind variability and initial wind vector—has been used to weight 24-hour predictions from both operations.

Weighting factors were obtained by dividing variability for the given initial wind (Fig. 13) by the average variability, 32.1 knots, of all data used in constructing the figure. This factor would be proportional to the difficulty of forecasting, and forecast errors thus were divided by this factor to provide relative weighting. Easy forecasts were strongly weighted; difficult forecasts were given less weight. Results, normalized to a unit-average weighting factor for each data set, are as follows:

TABLE III

Vector Standard Errors
(knots)

	1953		1955	
	Forecasts	Persistence	Forecasts	Persistence
No weighting*	39.8	42.2	30.0	30.7
Weighted	37.1	38.8	30.1	30.9

*Data from Table II.

The 1953 data show an improvement in results gained by objectively weighting forecasts but, in the 1955 data, a slight opposite effect is noted. On the other hand, the ratio of forecast to persistence errors is degraded by weighting in the 1953 data, and improves in the 1955 data. However, the improvement appears small. A larger sample should show a more significant effect of weighting, if it is possible to determine in advance which forecasts are most likely to succeed or fail.

Fallout Safety Probability Computations

Thus far, it has been shown that meteorological forecasts and persistence furnish almost equally useful wind predictions. Since many more data are available on persistence or wind changes, rules may be derived for variability which are equally valid when applied to forecast errors.

Variability is shown to be dependent upon time interval, altitude, season, and initial vector wind. Wind speed provides only a rough measure of subsequent change. It will be

assumed now that the basic pattern of springtime variability, determined by altitude and time interval as described by Eqs 3 and 4, will hold for other seasons and vector winds. Only an additional pair of coefficients would be required, one expressing the specific seasonal variability divided by springtime over-all variability, the other being the ratio of variability for the specific wind vector (Fig. 13) to the over-all average for springtime. Seasonal factors, obtained from all-level changes in Table I, are shown in Table IV.

TABLE IV

Seasonal Coefficients of Variability

Winter	1.346
Spring	1.000
Summer	0.779
Fall	0.804

Ratio contours for wind vectors are shown in Fig. 19, which is the same as Fig. 13 except that all values have been divided by 32.1 knots—the spring, all-level, standard deviation. A similar transformation for Fig. 14, summer data, is easily obtained without interpolation, since over-all 24-hour variability for the season is 25.0 knots. Thus, the 10 line of Fig. 14 would have a 0.40 proportion label; the 15 line, a 0.60 label, etc. In this manner, basic input charts (Ref 1) for a fallout safety probability calculation may be shifted by a constant value to account for synoptic type and season.

A forecasting proficiency coefficient may be applied in exactly the same way when a prediction system is found which yields a coefficient significantly smaller than 1.00.

As previously described (Ref 1), trajectory errors expected at briefing times (Ref 11)—from using wind data 2, 6, 12, and 24 hours old at shot time—have been numerically integrated by using Eq 4, which fits NTS spring data. Computed standard vector errors are shown in Table V, with the number of hours between wind-data time and particle-landing time at 4000-feet MSL. Calculations were made for 40-, 60-, 100-, and 200-micron-diameter particles originating at shot time at 10,000, 20,000, 30,000, 40,000 and 50,000 feet MSL. Although some of these values appear to be large, they barely approach an empirical limiting value of ±5 degrees latitude, noted by Buell (Ref 12). This value for temperate latitudes in the U.S. was determined from trajectories of constant-level transosonde balloons (Ref 13).

TABLE V

Hours From Wind Observation Until Time Particle Lands at 4000 MSL, ΔT, and Trajectory Standard Vector Error*, σ.

Initial altitude (kft MSL)	Wind observation time (hours)	Particle diameter (microns) 40 σ	40 ΔT	60 σ	60 ΔT	100 σ	100 ΔT	200 σ	200 ΔT
10	H-2	9.0	5.2	4.8	3.9	2.2	2.9	0.8	2.4
	H-6	13.4	9.2	7.5	7.9	3.7	6.9	1.4	6.4
	H-12	18.1	15.2	10.3	13.9	5.1	12.9	2.0	12.4
	H-24	25.1	27.2	14.4	25.9	7.2	24.9	2.9	24.4
20	2	35.9	10.6	18.2	7.0	8.1	4.5	2.9	3.0
	6	48.7	14.6	26.4	11.0	12.6	8.5	4.8	7.0
	12	63.4	20.6	35.4	17.0	17.3	14.5	6.7	13.0
	24	85.4	32.6	48.5	29.0	24.1	26.5	9.4	25.0
30	2	86.6	16.0	42.9	10.1	18.6	6.1	6.5	3.6
	6	112.9	20.0	59.2	14.1	27.4	10.1	10.6	7.6
	12	143.3	26.0	79.2	20.1	38.2	16.1	14.7	13.6
	24	190.5	38.0	107.5	32.1	53.0	28.1	20.6	25.6
40	2	141.2	21.3	68.0	13.2	28.2	7.6	9.4	4.2
	6	172.5	25.3	89.1	17.2	40.5	11.6	14.8	8.2
	12	210.9	31.3	113.7	23.2	53.8	17.6	20.4	14.2
	24	272.0	43.3	151.4	35.2	73.6	29.6	28.4	26.2
50	2	194.7	26.7	91.8	16.4	37.0	9.2	11.8	4.8
	6	227.6	30.7	114.6	20.4	50.6	13.2	18.0	8.8
	12	269.6	36.7	142.0	26.4	65.8	19.2	24.7	14.8
	24	338.2	48.7	185.1	38.4	88.8	30.2	32.5	26.8

*Nautical miles

These values, divided into particle fall times, give an input to a fallout safety probability estimate (Ref 1). Rather than repeat the previous method, which assumed that error components perpendicular to the predicted trajectory would be normally distributed, a circular bivariate normal distribution was used. Probabilities were calculated, using tables of the bivariate normal distribution recently published by Owen (Ref 14). A new computer chart, which incorporates NTS data and a further calculation stage for season or wind vector (or forecast capability, if available) coefficient, is shown in Fig. 20.

Use of this chart can be illustrated by an example of computing fallout safety probability: Assume that a predicted test fallout pattern indicates that the maximum extent of the 4-r contour is associated with 60-micron particles falling from 30,000 feet MSL. The prediction is

based on a wind observation made 6 hours before shot time, when the mean wind speed from the surface to 30,000 feet was 20 knots. Also, the shot was made in summer, and the 30,000-foot-MSL observed wind was from 200 degrees at 56 knots. Finally, the predicted pattern lay down the middle of a 30-degree safe sector.

First, the seasonal coefficient for summer (Table IV) is 0.779. The wind vector coefficient (Fig. 14) for the given 30,000-foot wind is 1.4. The product of these two coefficients is k = 1.09. In Fig. 20, where the H-6-hour chart shows that for 60-micron particles falling from 30,000 feet MSL, $T/\sigma_y = 0.193$. Follow the 0.193 line across to the 1.09 line on the coefficient graph to show an adjusted $T/\sigma_y = 0.175$. Then follow the 0.175 line down to the wind chart to an intersection with the 20-knot line at $\frac{WT}{\sqrt{2}\, k\sigma_y} = 2.5$.

Next, follow the 2.5 line across to the sector angle width chart to the 15-degree curve (±15 degrees safe sector width), giving a probability of 26 percent that the particles described will land within 15 degrees on one side of the predicted position. Thus, there is a 52 percent probability of these particles landing in the 30-degree sector.

Summary

Nevada Test Site winds-aloft records have been studied to determine how wind changes with time at that location. Results are:

1. General agreement with other investigations was found, but variability is somewhat greater than has been observed in Southern California.

2. These data appear to confirm prior estimates that wind changes are proportional to the square root of the time interval, at least to 24-hour intervals.

3. Wind variability increases with altitude to a maximum near 30,000 or 35,000 feet MSL near the tropopause and decreases above that level. This pattern is borne out during all four seasons.

4. Upper air variability is greatest in winter, least in summer. At low levels, little seasonal difference was noted.

5. Vector wind changes are related to wind speeds; however, the correlation seems to be weak and may be neglected.

6. A systematic pattern has been derived to relate variability to wind vector and, thus, 'type' variability conditions. Variability ranges from 1/2 to 3 times the seasonal normal, depending on the initial 30,000-foot-MSL wind vector.

7. Forecasting errors made at NTS have nearly the same magnitude and distribution as errors which would have been made by assuming persistence of latest observations available at forecast delivery time.

8. A new fallout safety probability calculator chart has been prepared from NTS data allowing use of parameters for season, weather type, and forecasting capability.

Additional Notes

Before this report could be edited and published, it was put to work at Operation PLUMBBOB. After a considerable workout, several pertinent comments have been found necessary. Of course, since the 1957 test operation was conducted mainly in the summer months, the statistics are not so valid and well-defined as they would have been for the spring months. No real objection to the representativeness of the data was noted, however. The general description of summer wind conditions, as reported, appears to have been verified.

PLUMBBOB weather and fallout briefings did not continue to refer primarily to the safe angular sectors which had been defined on previous operations. Thus, a safety probability computation, as described by this report, was not often used. Instead, the calculator (Fig. 20) was often used to obtain probabilities that various dose contours would contain specific villages. Also, for nearly every shot briefing, 50- and 90-percent probable errors in forecast hot-line bearing were calculated from the report and presented during the advisory panel discussion of the briefing.

One notable difficulty became apparent in these applications. Whenever a large direction shift was forecast, the range of errors to be expected from assuming persistence did not conform to the range of errors expected from past forecast capability. Yet the probable error from both forecast systems is almost the same. No survey of PLUMBBOB data has been attempted to find some weighting process for considering both forecasts, as was done for UPSHOT-KNOTHOLE data (Refs 15 and 16). U.S. Weather Bureau and Air Weather Service personnel performed some verification studies of PLUMBBOB forecasts, but neither group has provided exactly the same data comparisons used in this report. There are indications that no radical improvement was effected, but final judgment must await adequate study of the data.

Also, it should be noted here that Mr. Frank Cluff performed a study,* under U.S. Weather Bureau-AEC sponsorship, of the same NTS data used in this report. The main emphasis was placed on wind speed and direction variability and the influence of wind observations made over very thick layers. Discussions between both investigators failed to yield any significant differences in either numerical results or general conclusions.

---

*Mr. Cluff's report is currently in process of publication; those interested in his results should request it from U.S. Weather Bureau, Office of Meteorological Research, Special Projects Section, Washington 25, D.C.

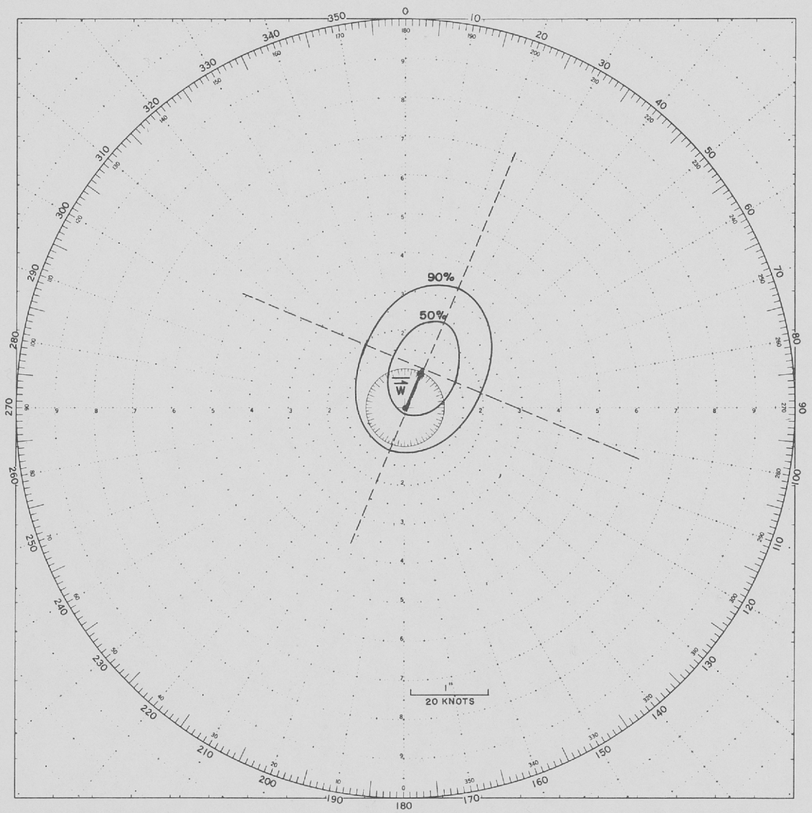

a. 700 millibars (10,000 ft MSL)

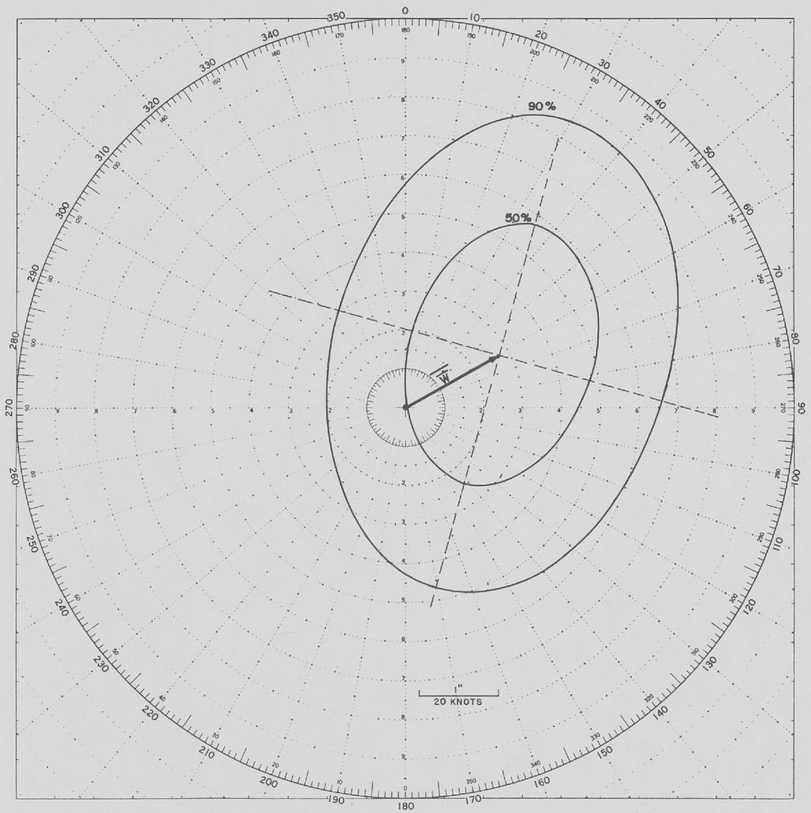

b. 300 millibars (30,000 ft MSL)

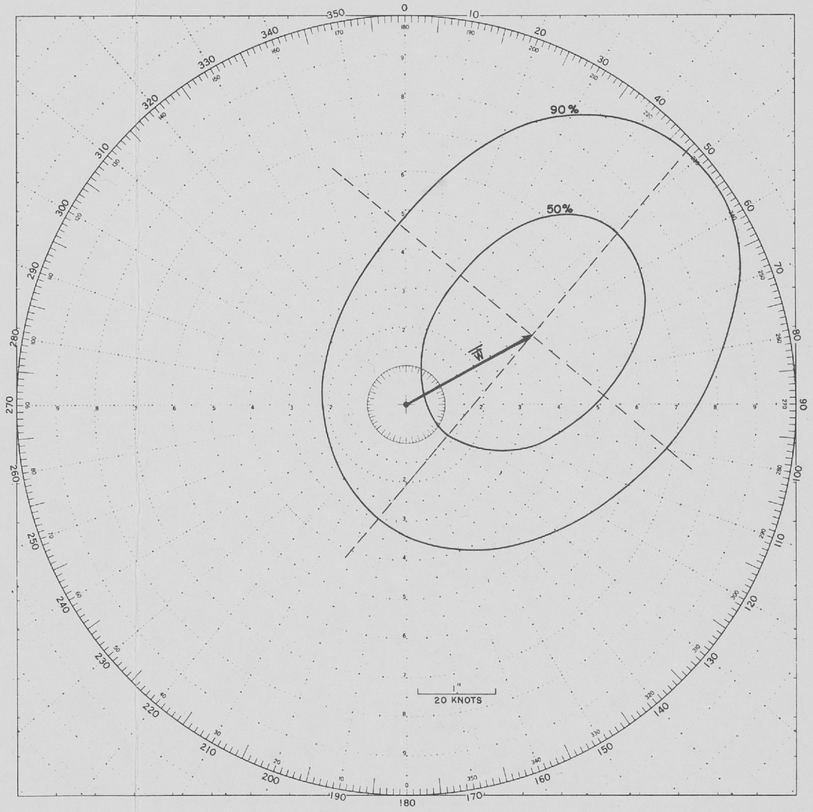

c. 200 millibars (40,000 ft MSL)

Fig. 1 -- Standard vector deviation wind rose, Las Vegas (summer)

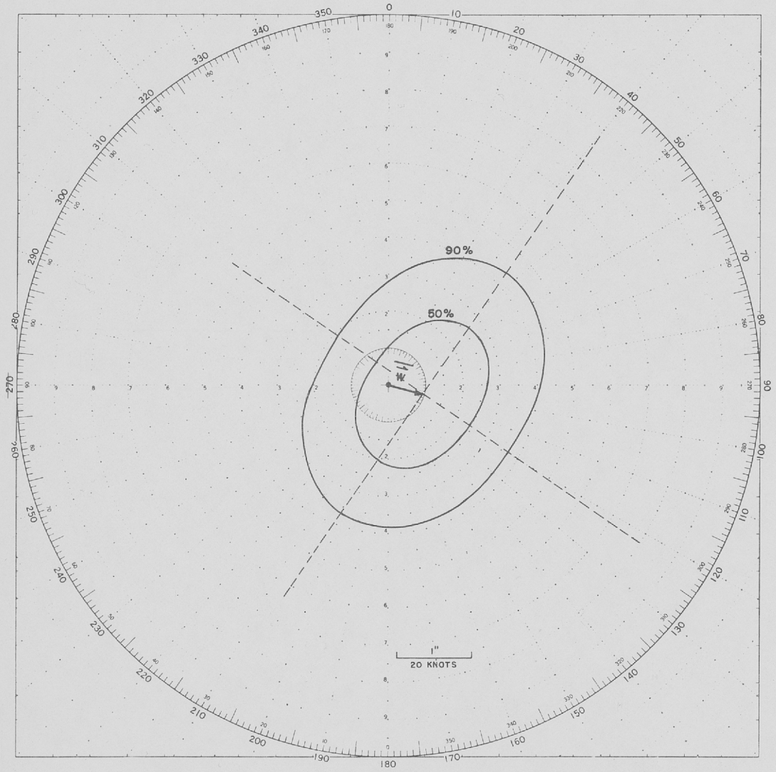

a. 700 millibars (30,000 ft MSL)

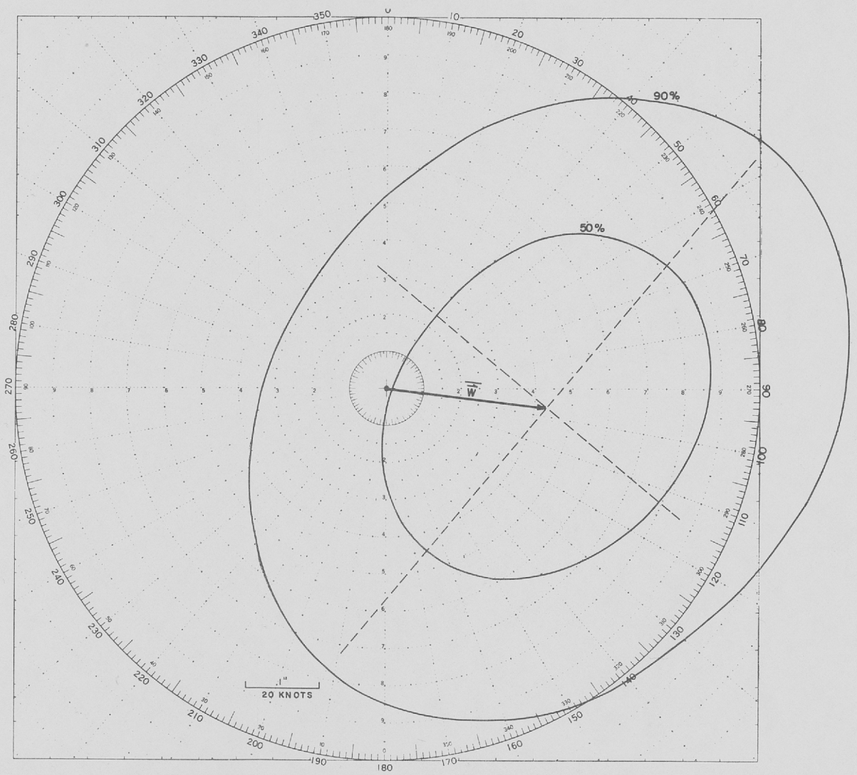

b. 300 millibars (30,000 ft MSL)

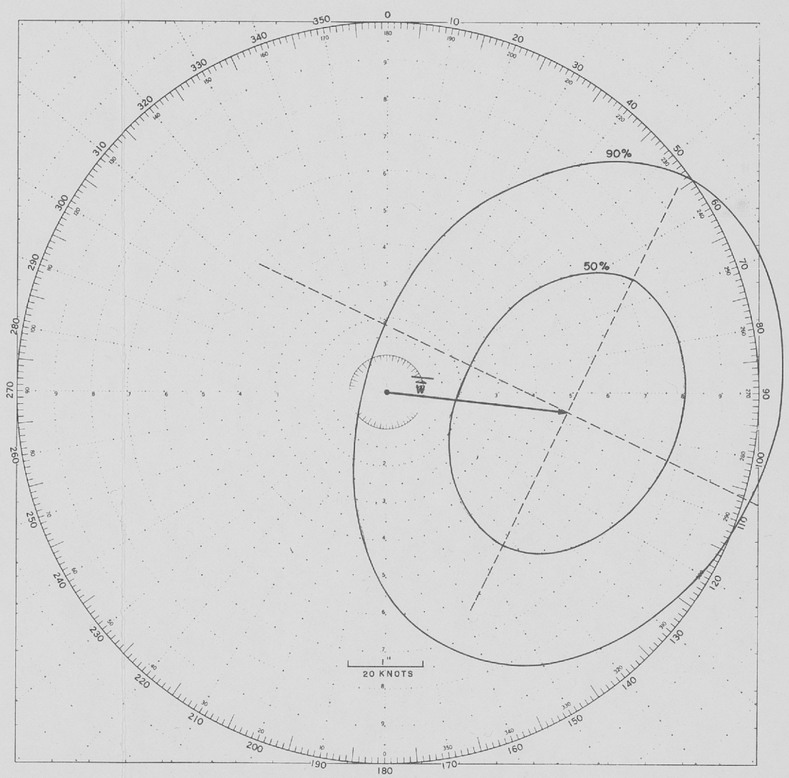

c. 200 millibars (40,000 ft MSL)

Fig. 2 -- Standard vector deviation wind rose, Las Vegas (winter)

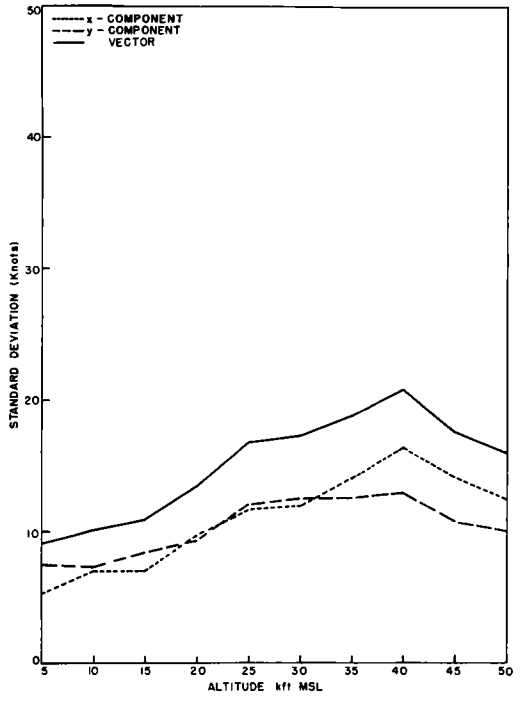

a. 3-hour time interval

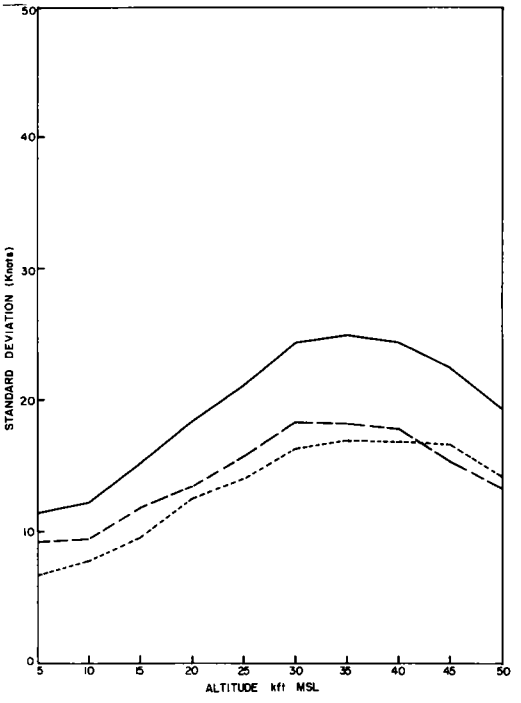

b. 6-hour time interval

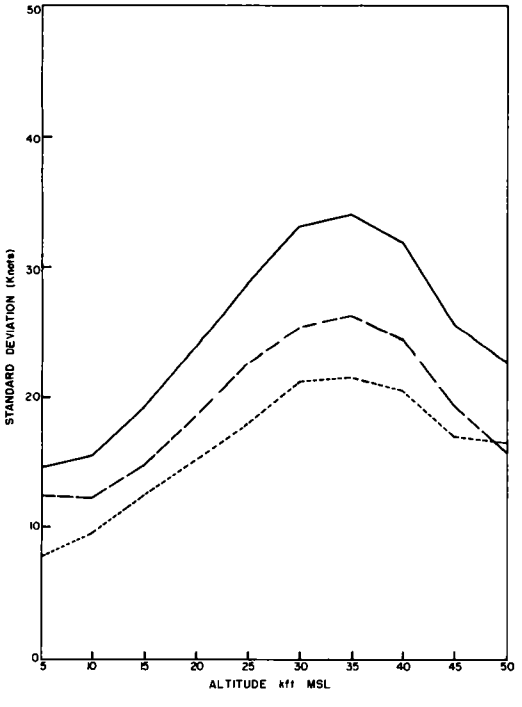

c. 12-hour time interval

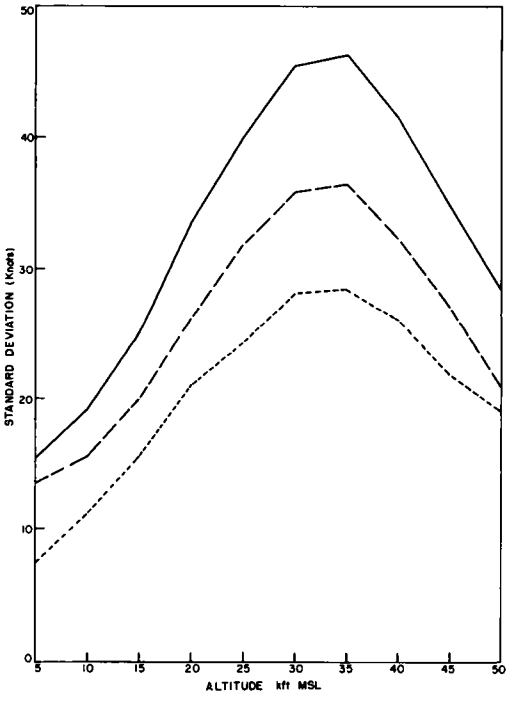

d. 12-hour time interval

Fig. 3 -- Spring wind variability

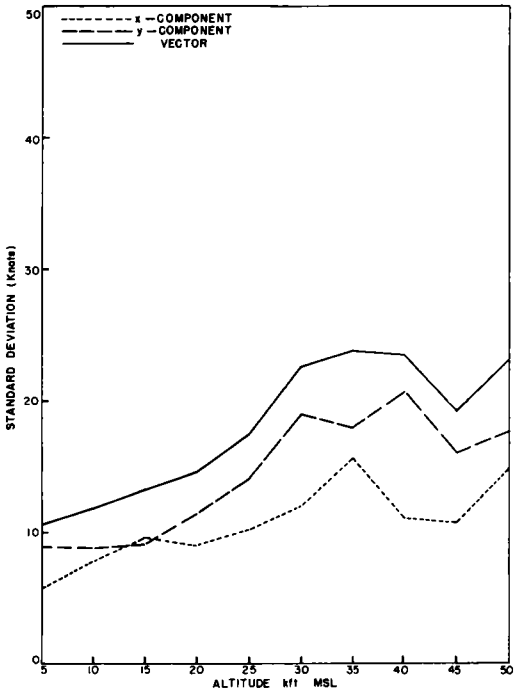

a. 6-hour time interval

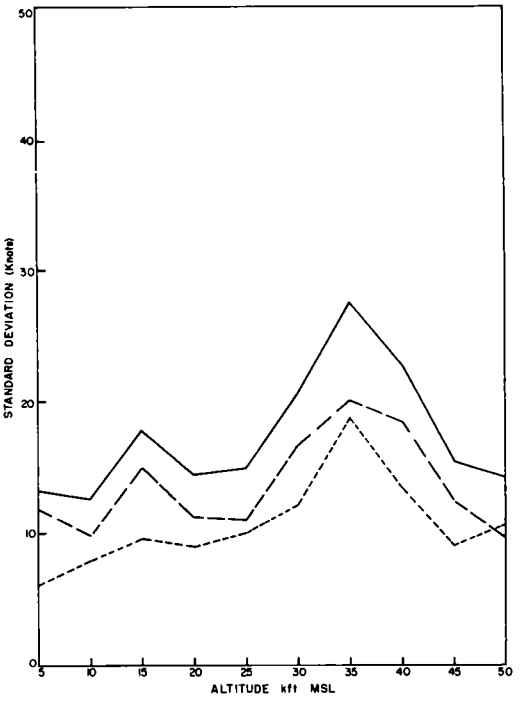

b. 12-hour time interval

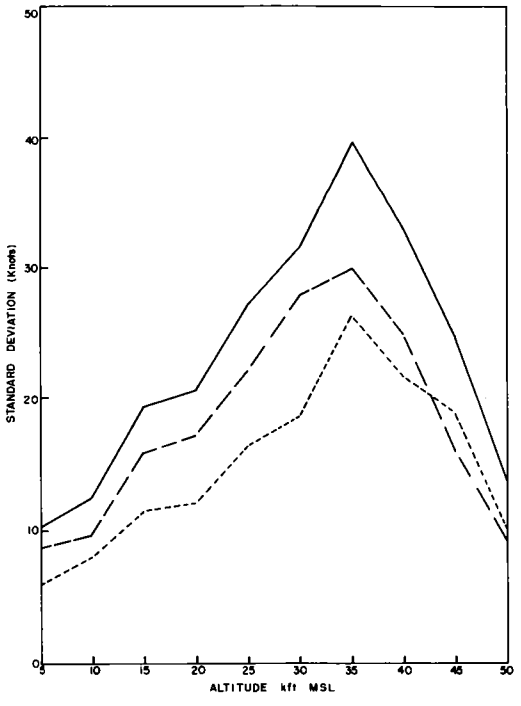

c. 24-hour time interval

Fig. 4 -- Summer wind variability

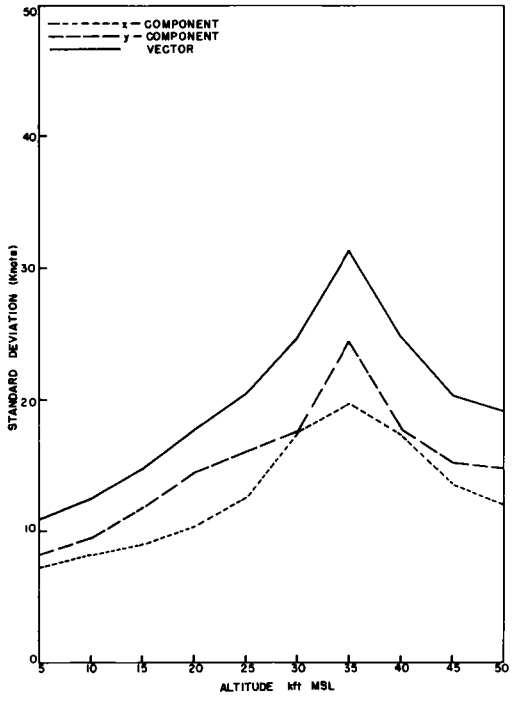

a. 12-hour time interval

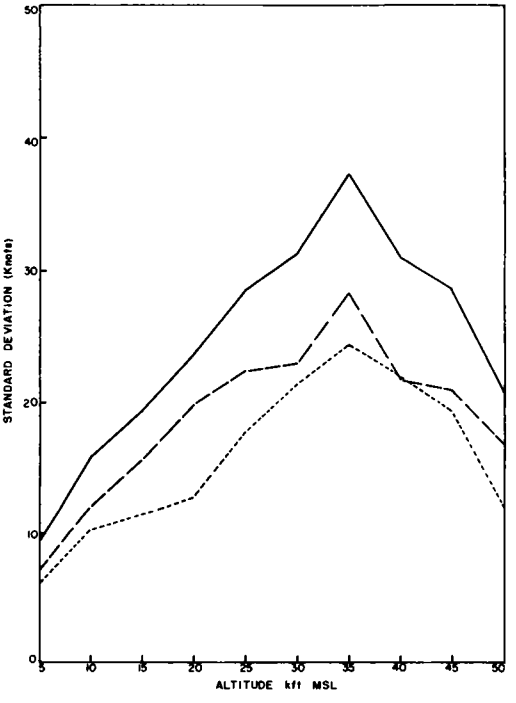

b. 24-hour time interval

Fig. 5 -- Fall wind variability

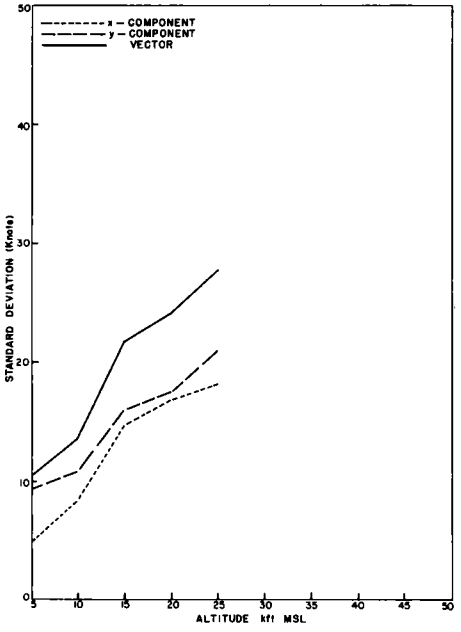

a. 6-hour time interval

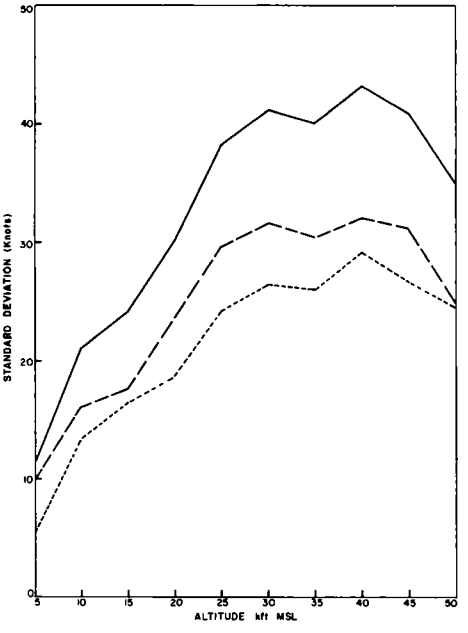

b. 12-hour time interval

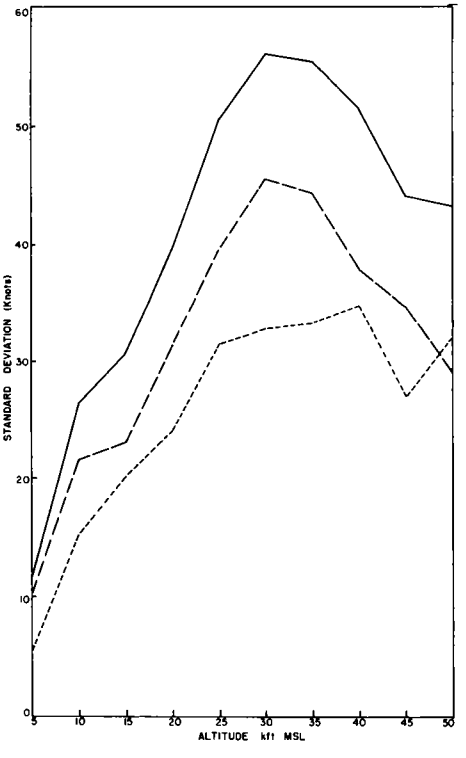

c. 24-hour time interval

Fig. 6 -- Winter wind variability

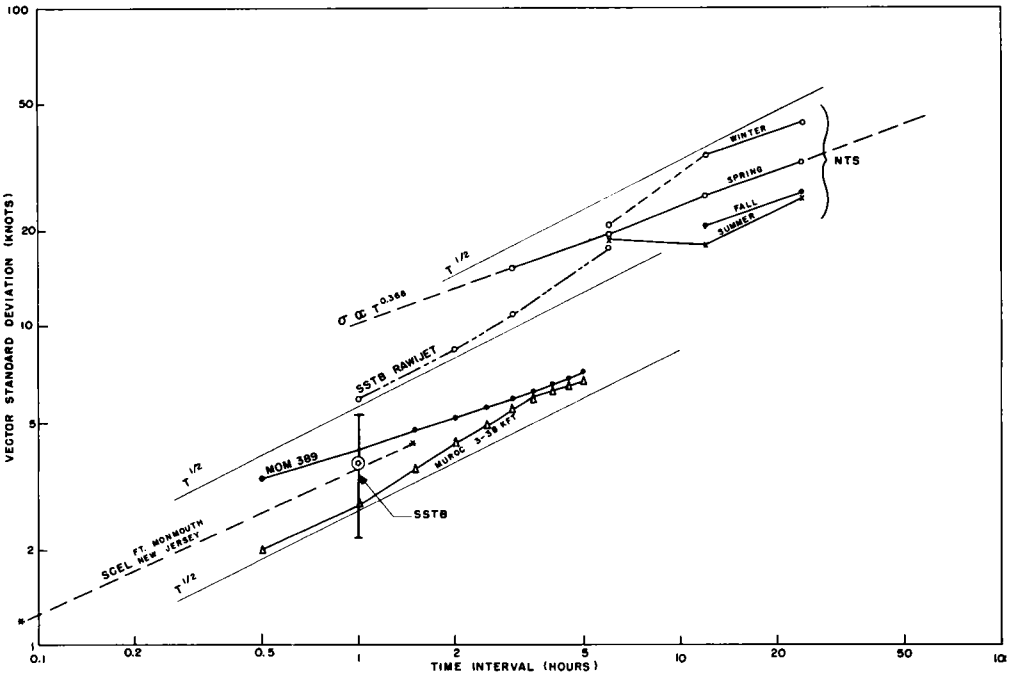

Fig. 7 -- Wind variability comparisons

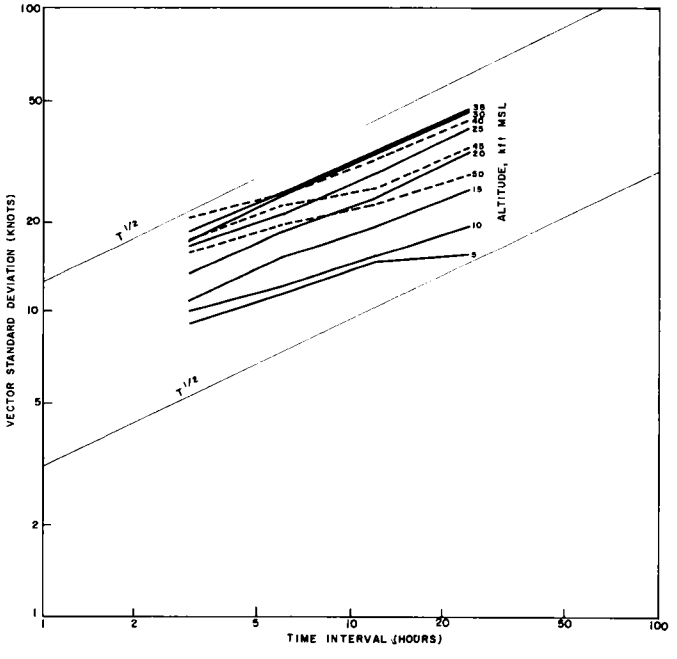

Fig. 8 -- Time variability versus altitude relation (spring)

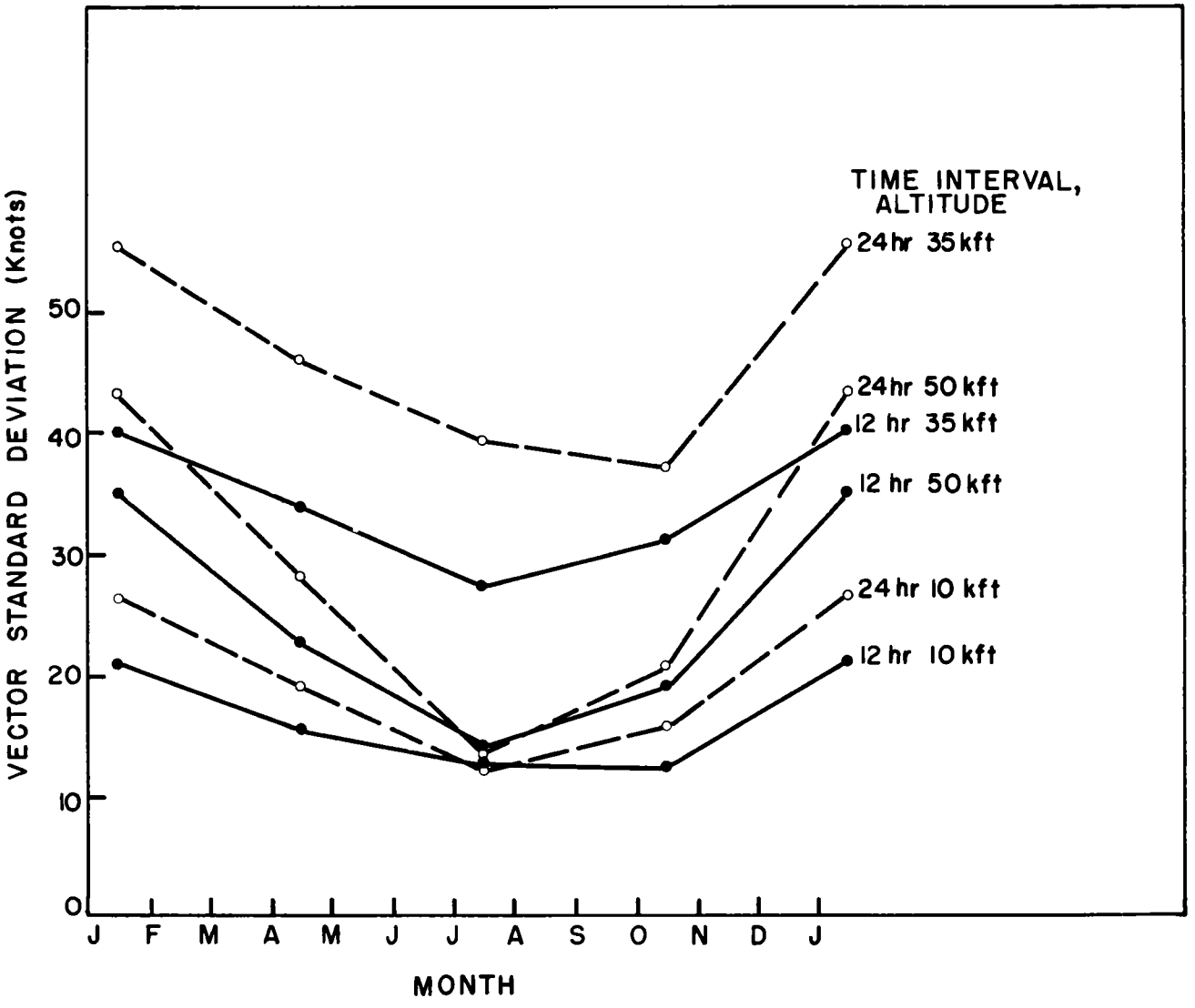

Fig. 9 -- Annual march of wind variability

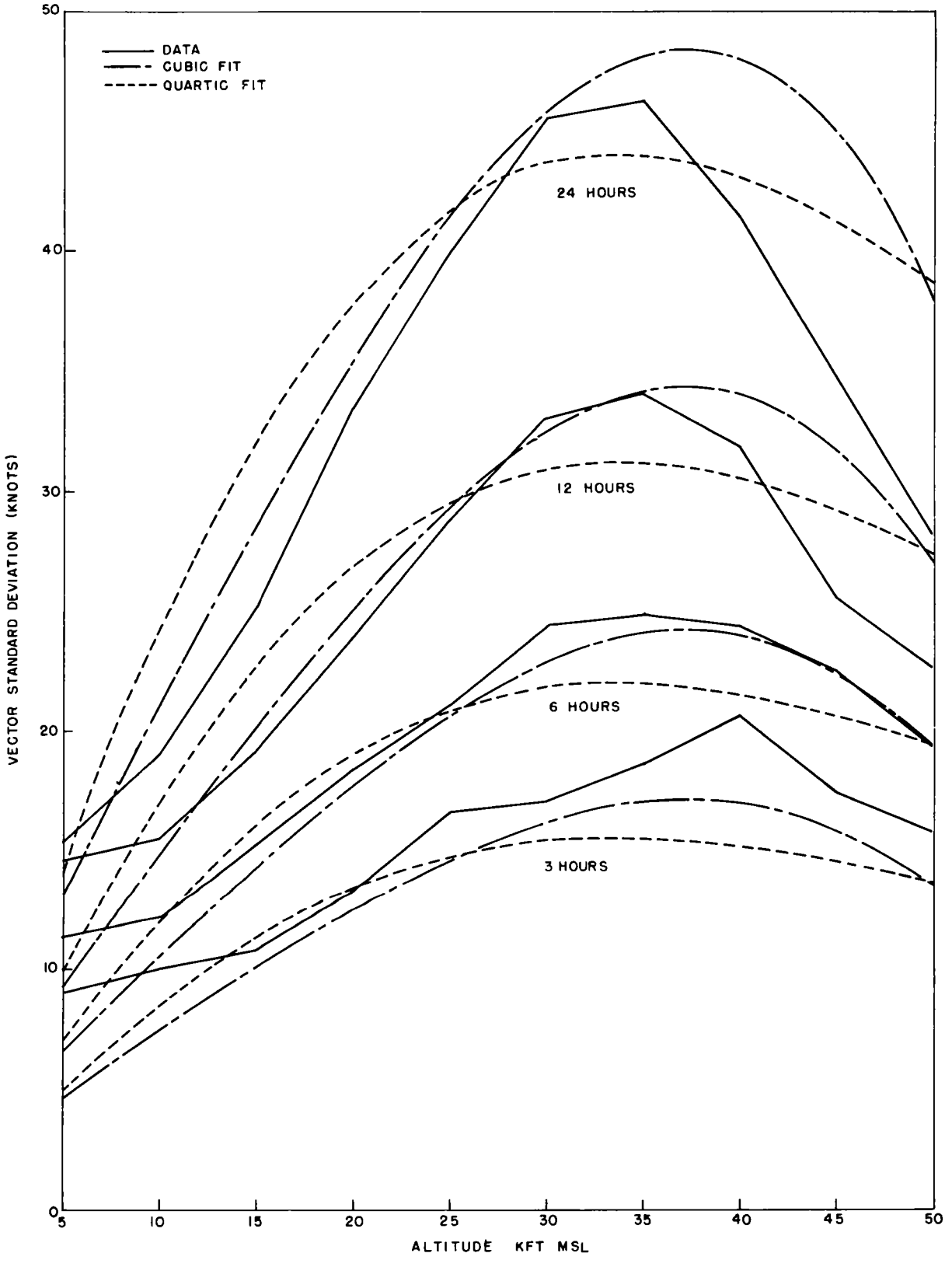

Fig. 10 -- Wind change versus altitude relation (spring)

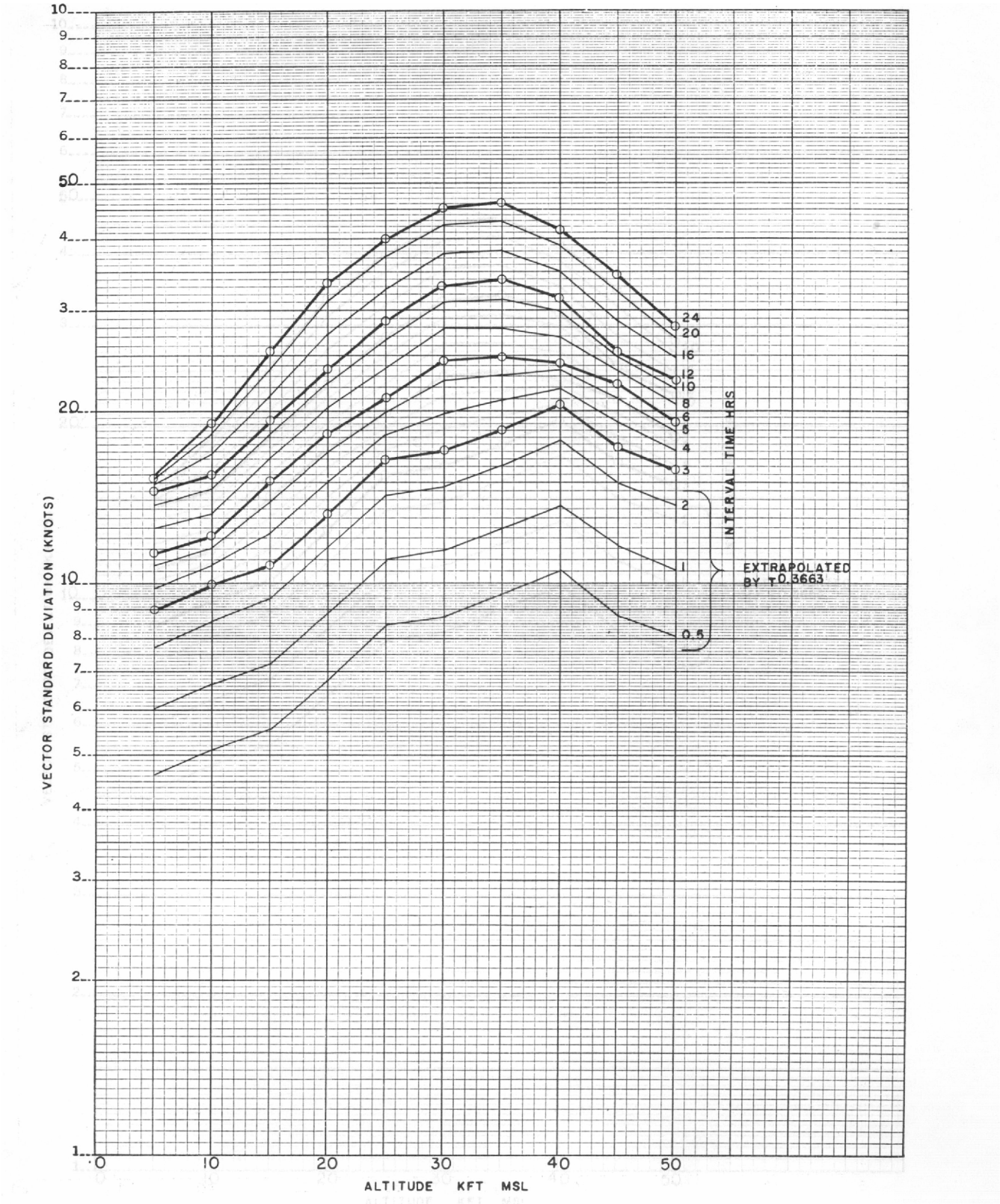

Fig. 11 -- Interpolation chart for wind variability (spring)

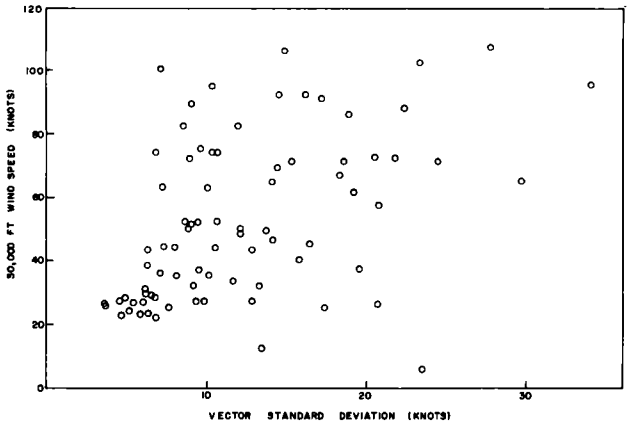

a. 3-hour time interval

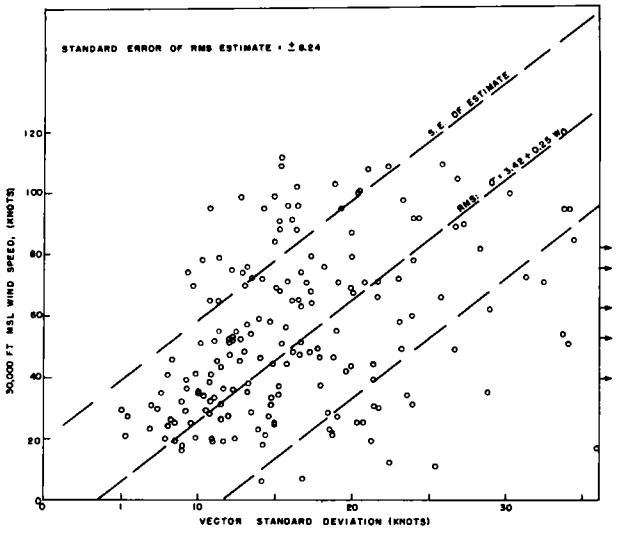

b. 6-hour time interval

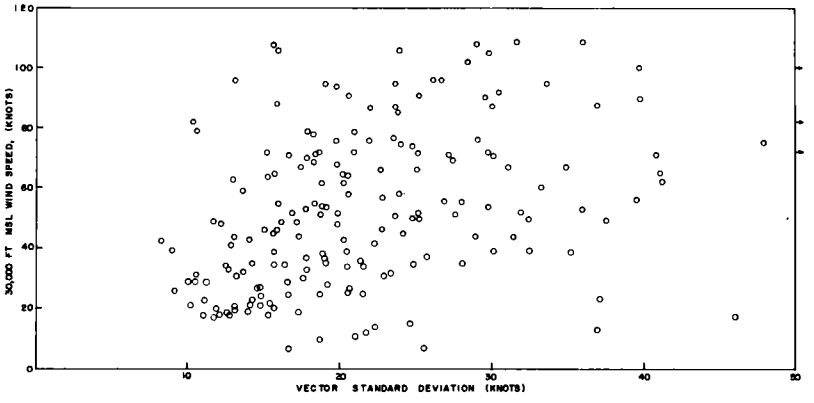

c. 12-hour time interval

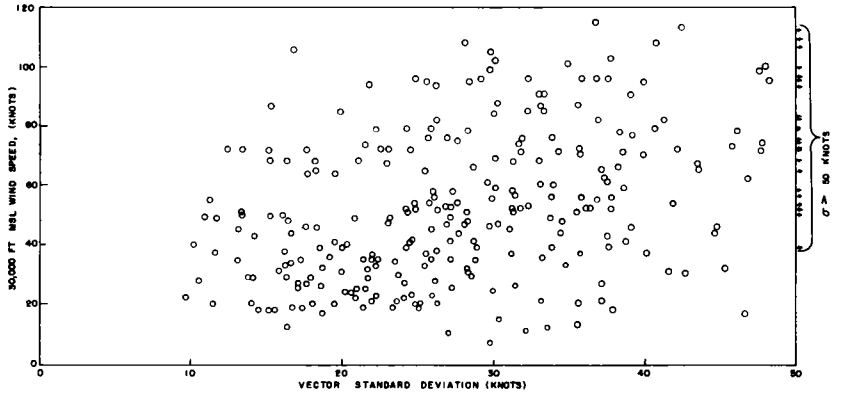

d. 24-hour time interval

Fig. 12 -- Wind speed versus variability (spring)

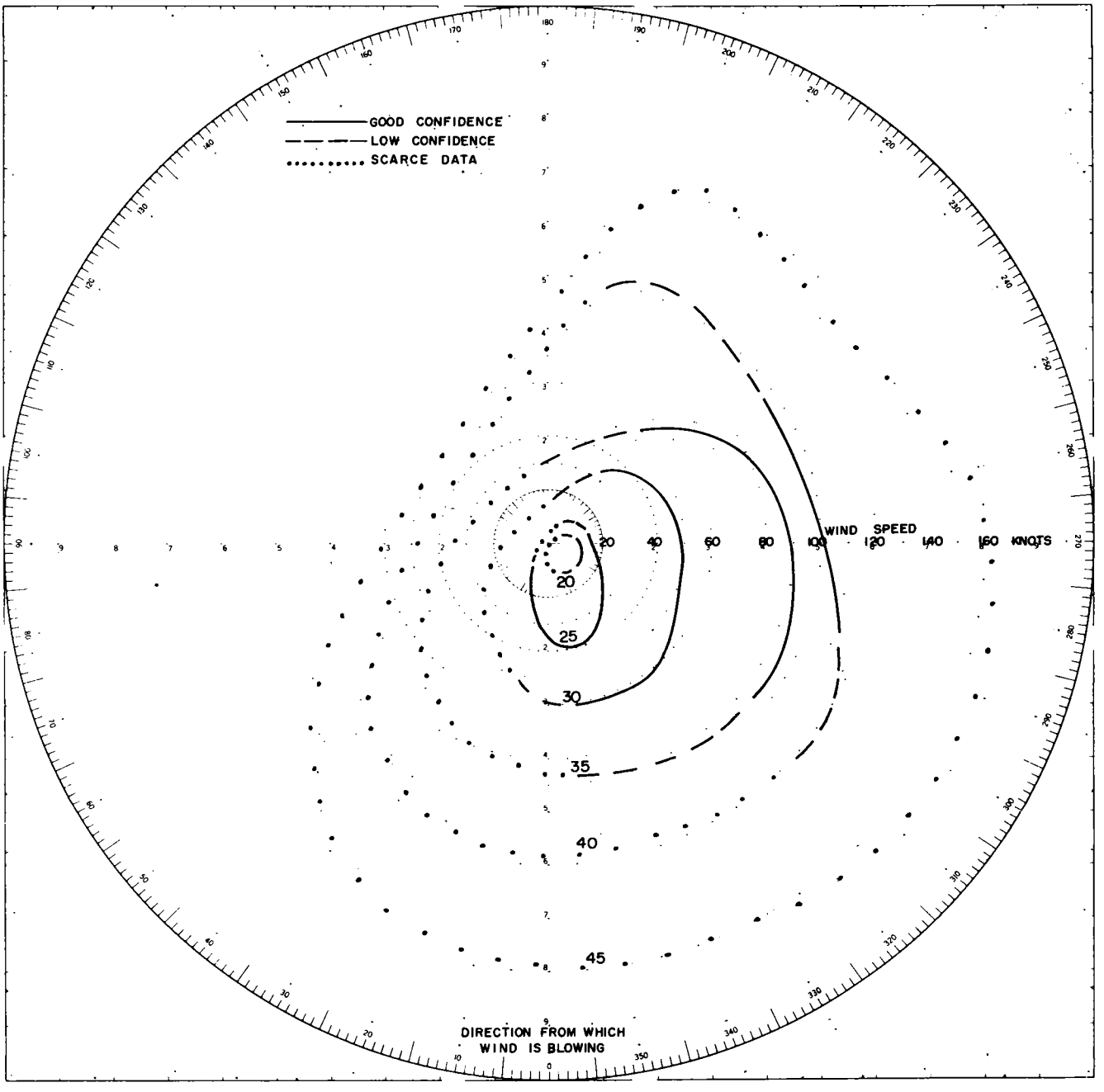

Fig. 13 -- Mercury 24-hour vector standard deviation for 30,000-foot-MSL wind vectors (spring)

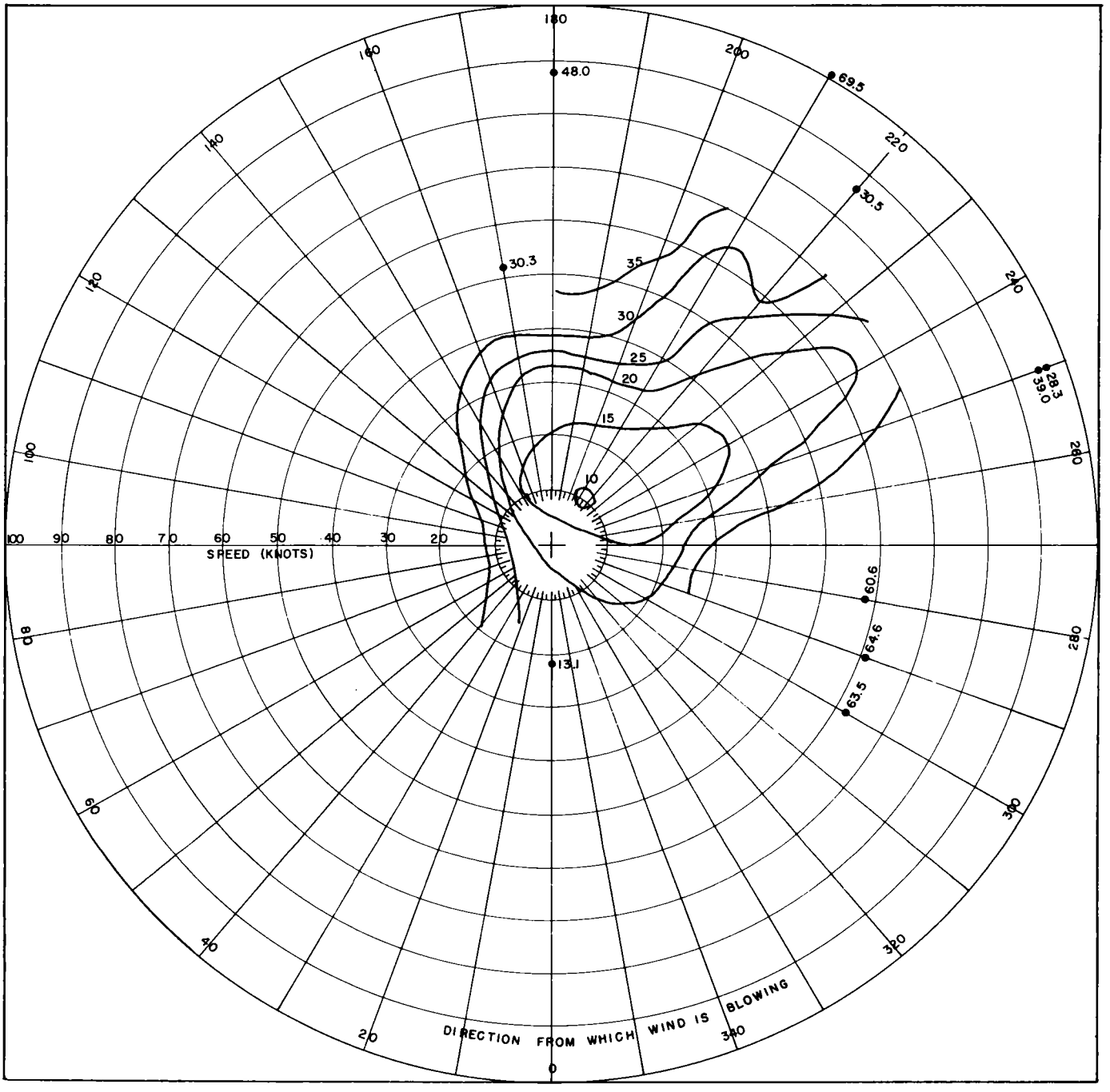

Fig. 14 -- Mercury 24-hour vector variability for 30,000-foot-MSL wind vectors (summer)

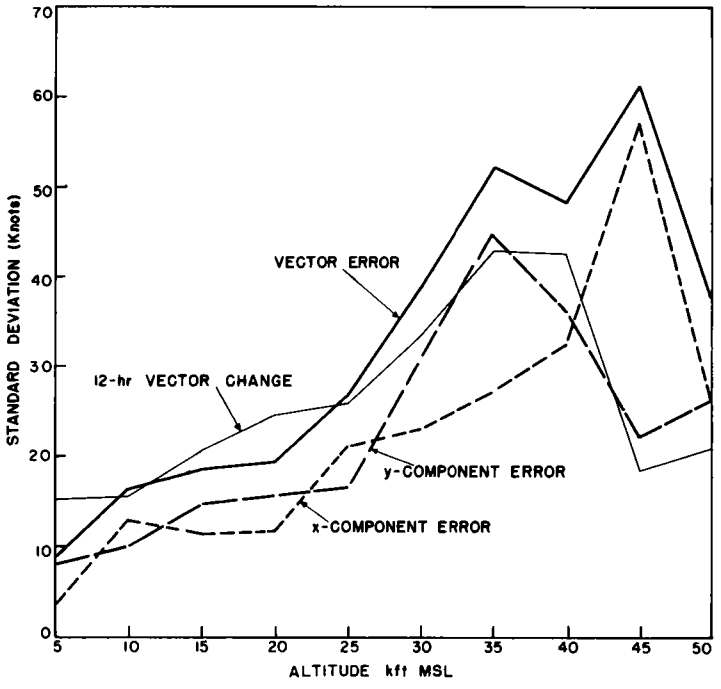

a. 12-hour forecasts

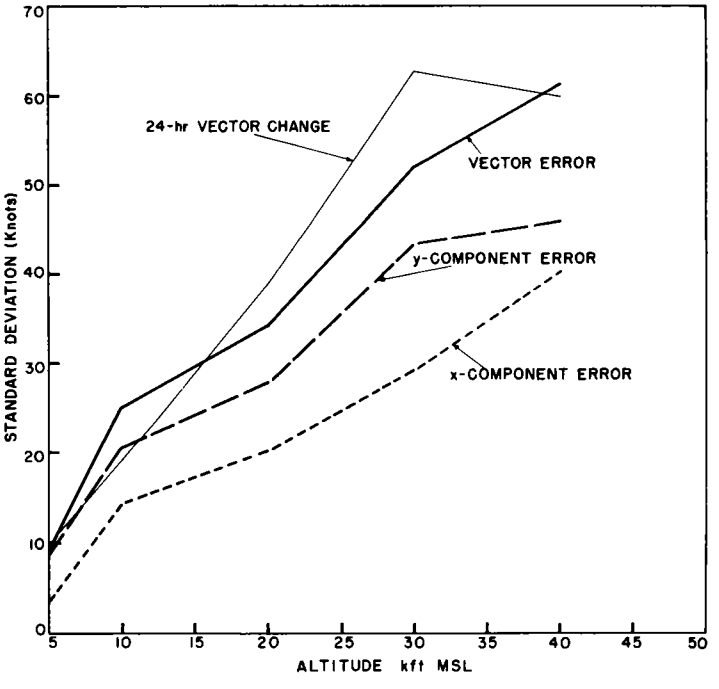

b. 24-hour forecasts

Fig. 15 -- UPSHOT-KNOTHOLE wind forecast errors

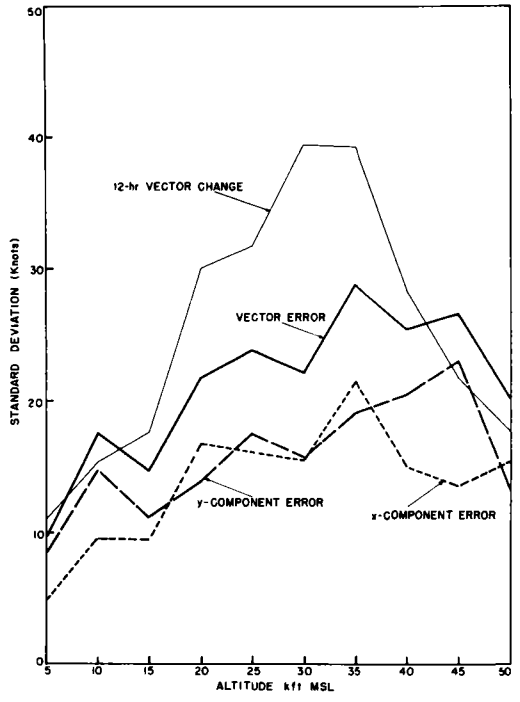

a. 12-hour forecasts

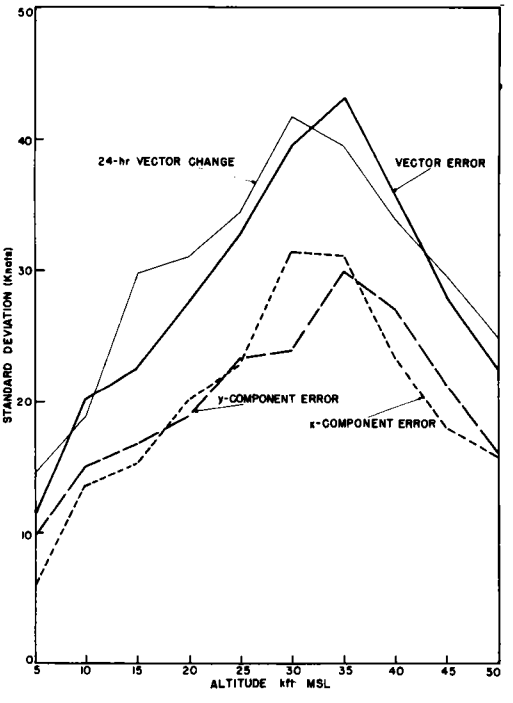

b. 24-hour forecasts

Fig. 16 -- TEAPOT wind forecast errors

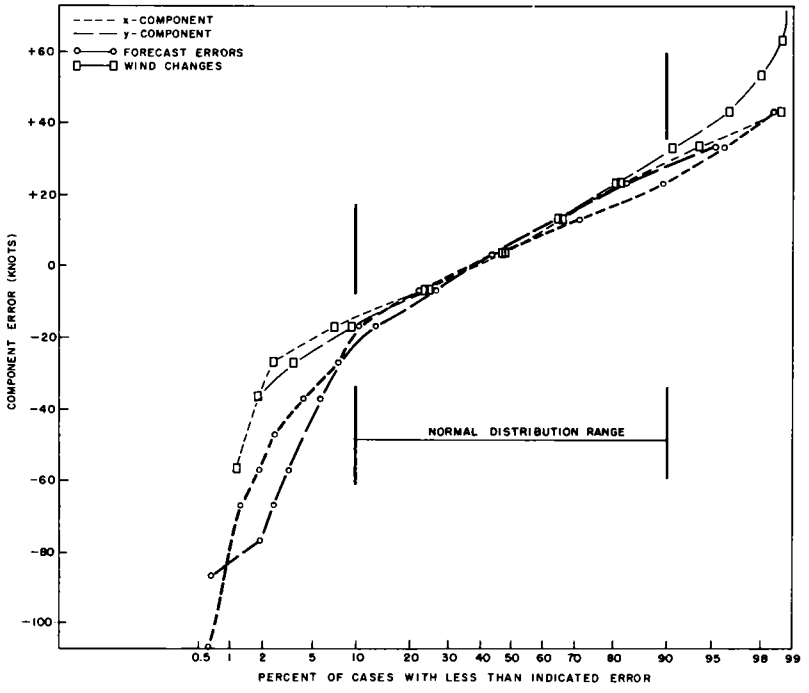

Fig. 17 -- Component error distribution, 1953 (12-hr)

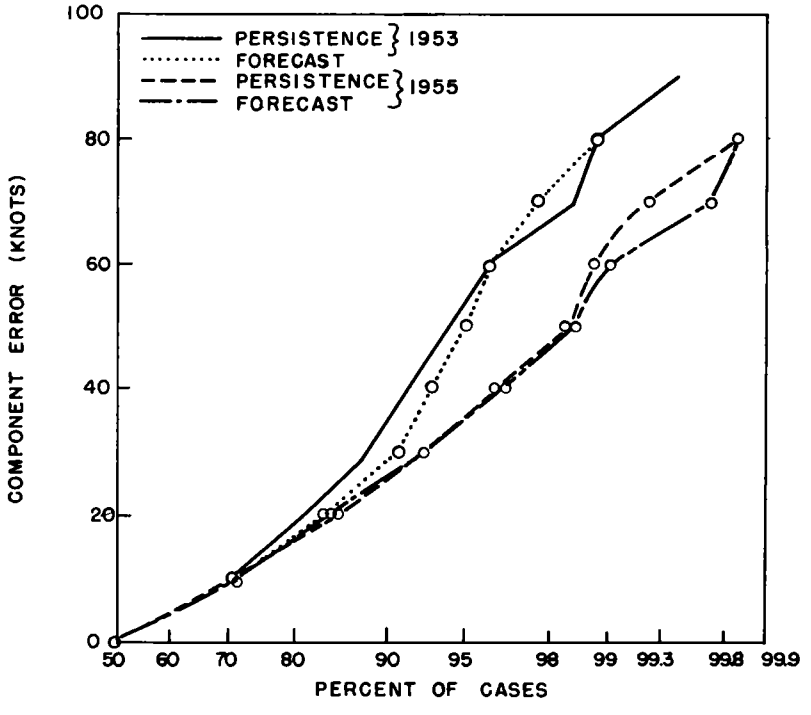

Fig. 18 -- Wind component error distribution (24-hr)

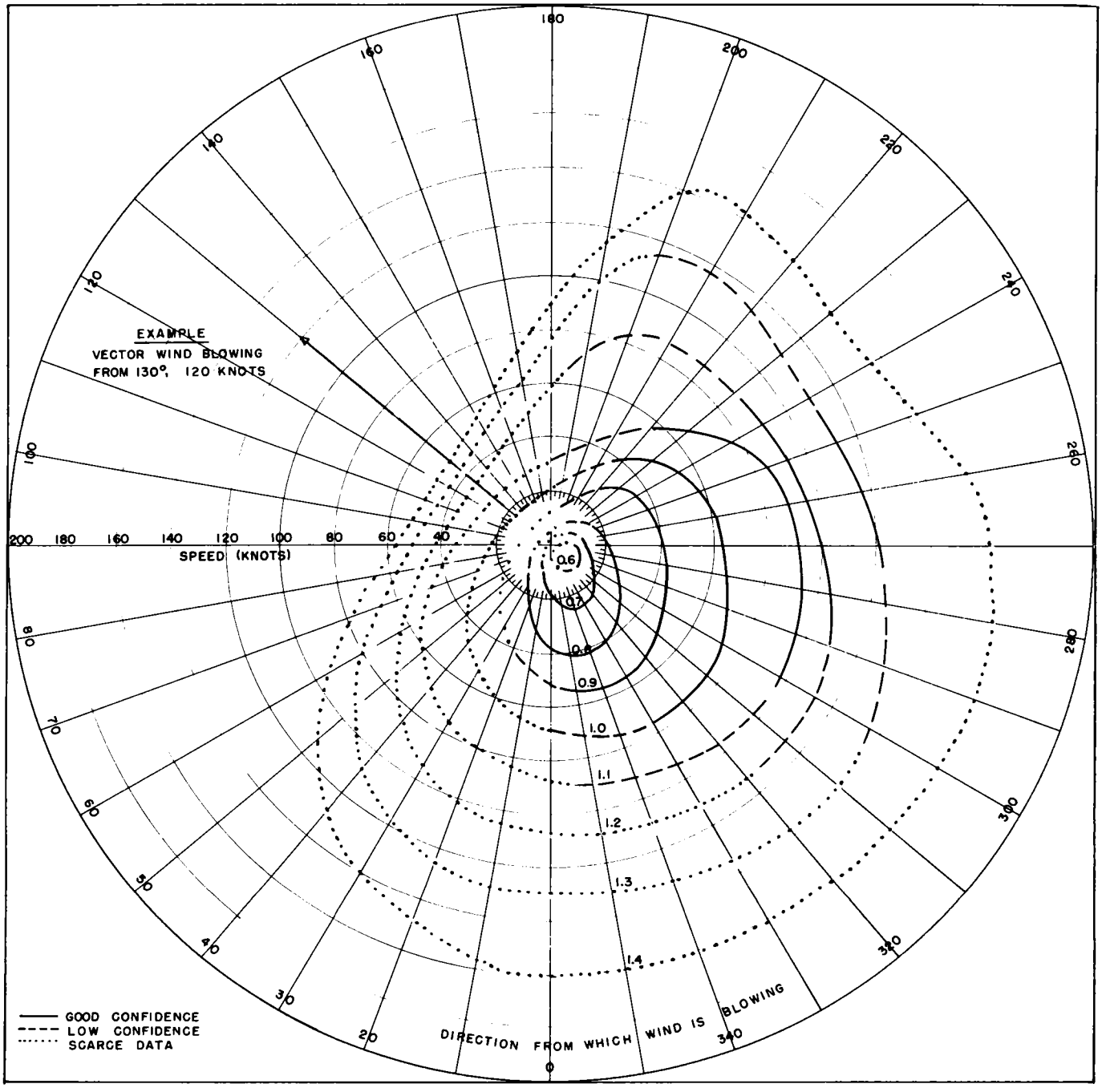

Fig. 19 -- Mercury 24-hour vector variability proportion of standard 32.1-knot deviation for 30,000-foot-MSL wind vectors (spring)

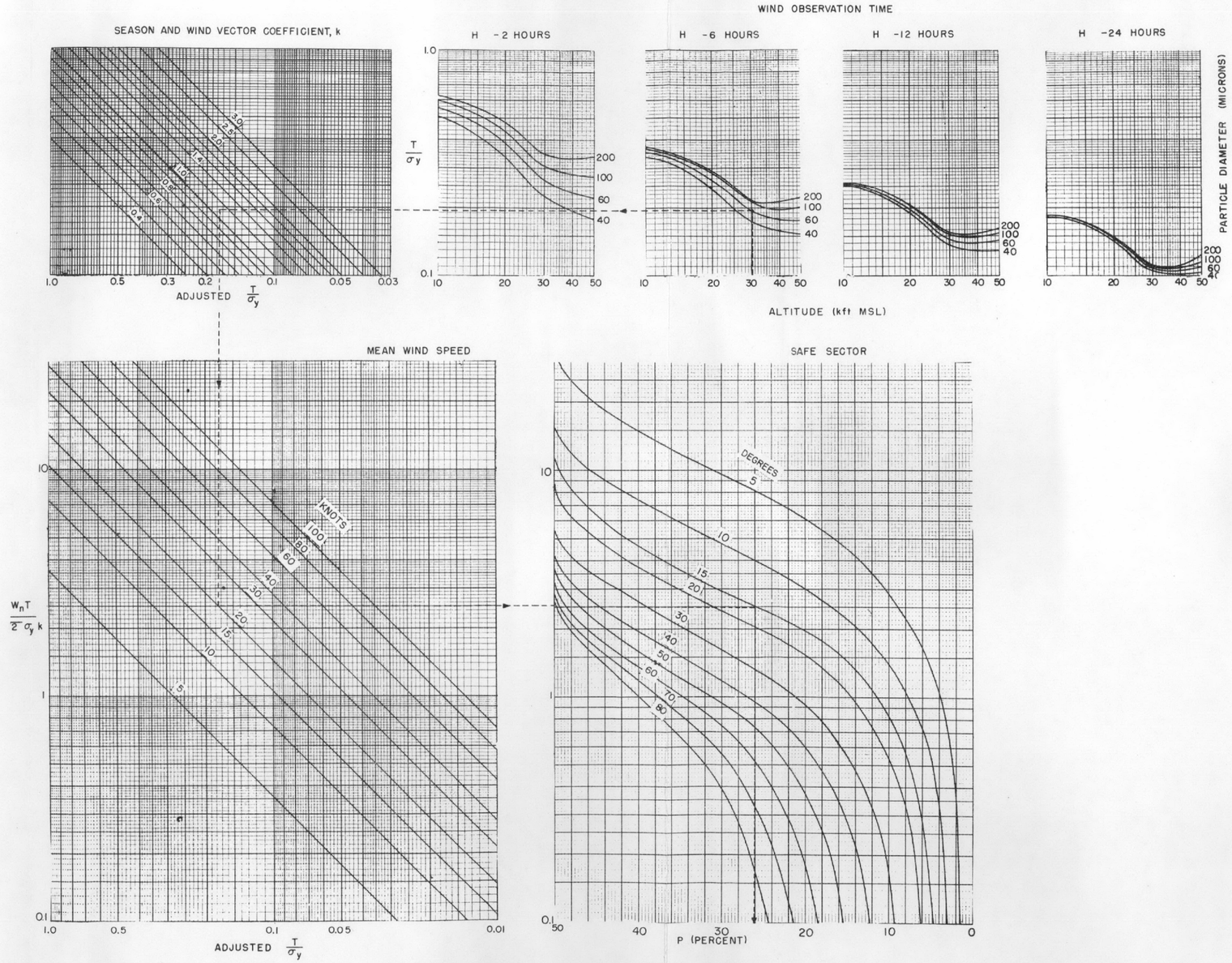

Fig. 20 -- Fallout safety probability computation chart

APPENDIX A

TABLES FOR COMPUTING WIND DISTRIBUTION STATISTICS

TABLE A-I

Table for Resolving Polar Coordinate Wind Observations to X (west-east) and Y (south-north) Component Winds

(W_x, W_y)

Direction from which wind blows (degrees)

Use sign									
(+, -)	360	350	340	330	320	310	300	290	280	270
(+, +)	180	190	200	210	220	230	240	250	260	270
(-, +)	180	170	160	150	140	130	120	110	100	90
(-, -)	0	10	20	30	40	50	60	70	80	90

Wind speed

1	0	1	0	1	0	1	0	1	1	1	1	1	1	0	1	0	1	0	1	0
2	0	2	0	2	1	2	1	2	1	2	2	1	2	1	2	1	2	0	2	0
3	0	3	1	3	1	3	2	3	2	2	2	2	3	2	3	1	3	1	3	0
4	0	4	1	4	1	4	2	3	3	3	3	3	3	2	4	1	4	1	4	0
5	0	5	1	5	2	5	2	4	3	4	4	3	4	2	5	2	5	1	5	0
6	0	6	1	6	2	6	3	5	4	5	5	4	5	3	6	2	6	1	6	0
7	0	7	1	7	2	7	4	6	5	5	5	5	6	4	7	2	7	1	7	0
8	0	8	1	8	3	8	4	7	5	6	6	5	7	4	8	3	8	1	8	0
9	0	9	2	9	3	8	4	8	6	7	7	6	8	4	8	3	9	2	9	0
10	0	10	2	10	3	9	5	9	6	8	8	6	9	5	9	3	10	2	10	0
11	0	11	2	11	4	10	6	10	7	8	8	7	10	6	10	4	11	2	11	0
12	0	12	2	12	4	11	6	10	8	9	9	8	10	6	11	4	12	2	12	0
13	0	13	2	13	4	12	6	11	8	10	10	8	11	6	12	4	13	2	13	0
14	0	14	2	14	5	13	7	12	9	11	11	9	12	7	13	5	14	2	14	0
15	0	15	3	15	5	14	8	13	10	11	11	10	13	8	14	5	15	3	15	0
16	0	16	3	16	5	15	8	14	10	12	12	10	14	8	15	5	16	3	16	0
17	0	17	3	17	6	16	8	15	11	13	13	11	15	8	16	6	17	3	17	0
18	0	18	3	18	6	17	9	16	12	14	14	12	16	9	17	6	18	3	18	0
19	0	19	3	19	6	18	10	16	12	15	15	12	16	10	18	6	19	3	19	0
20	0	20	3	20	7	19	10	17	13	15	15	13	17	10	19	7	20	3	20	0
21	0	21	4	21	7	20	10	18	14	16	16	14	18	10	20	7	21	4	21	0
22	0	22	4	22	8	21	11	19	14	17	17	14	19	11	21	8	22	4	22	0
23	0	23	4	23	8	22	12	20	15	18	18	15	20	12	22	8	23	4	23	0
24	0	24	4	24	8	23	12	21	15	18	18	15	21	12	23	8	24	4	24	0
25	0	25	4	25	9	23	12	22	16	19	19	16	22	12	23	9	25	4	25	0
26	0	26	5	26	9	24	13	23	17	20	20	17	23	13	24	9	26	5	26	0
27	0	27	5	27	9	25	14	23	17	21	21	17	23	14	25	9	27	5	27	0
28	0	28	5	28	10	26	14	24	18	21	21	18	24	14	26	10	28	5	28	0
29	0	29	5	29	10	27	14	25	19	22	22	19	25	14	27	10	29	5	29	0
30	0	30	5	30	10	28	15	26	19	23	23	19	26	15	28	10	30	5	30	0
31	0	31	5	31	11	29	16	27	20	24	24	20	27	16	29	11	31	5	31	0
32	0	32	6	32	11	30	16	28	21	25	25	21	28	16	30	11	32	6	32	0
33	0	33	6	32	11	31	16	29	21	25	25	21	29	16	31	11	32	6	33	0
34	0	34	6	33	12	32	17	29	22	26	26	22	29	17	32	12	33	6	34	0
35	0	35	6	34	12	33	18	30	23	27	27	23	30	18	33	12	34	6	35	0
36	0	36	6	35	12	34	18	31	23	28	28	23	31	18	34	12	35	6	36	0
37	0	37	6	36	13	35	18	32	24	28	28	24	32	18	35	13	36	6	37	0
38	0	38	7	37	13	36	19	33	24	29	29	24	33	19	36	13	37	7	38	0
39	0	39	7	38	13	37	20	34	25	30	30	25	34	20	37	13	38	7	39	0
40	0	40	7	39	14	38	20	35	26	31	31	26	35	20	38	14	39	7	40	0
41	0	41	7	40	14	39	20	36	26	31	31	26	36	20	39	14	40	7	41	0
42	0	42	7	41	14	39	21	36	27	32	32	27	36	21	39	14	41	7	42	0
43	0	43	7	42	15	40	22	37	28	33	33	28	37	22	40	15	42	7	43	0
44	0	44	8	43	15	41	22	38	28	34	34	28	38	22	41	15	43	8	44	0
45	0	45	8	44	15	42	22	39	29	34	34	29	39	22	42	15	44	8	45	0
46	0	46	8	45	16	43	23	40	30	35	35	30	40	23	43	16	45	8	46	0
47	0	47	8	46	16	44	24	41	30	36	36	30	41	24	44	16	46	8	47	0
48	0	48	8	47	16	45	24	42	31	37	37	31	42	24	45	16	47	8	48	0
49	0	49	9	48	17	46	24	42	32	38	38	32	42	24	46	17	48	9	49	0
50	0	50	9	49	17	47	25	43	32	38	38	32	43	25	47	17	49	9	50	0
51	0	51	9	50	17	48	26	44	33	39	39	33	44	26	48	17	50	9	51	0
52	0	52	9	51	18	49	26	45	33	40	40	33	45	26	49	18	51	9	52	0
53	0	53	9	52	18	50	26	46	34	41	41	34	46	26	50	18	52	9	53	0
54	0	54	9	53	18	51	27	47	35	41	41	35	47	27	51	18	53	9	54	0
55	0	55	10	54	19	52	28	48	35	42	42	35	48	28	52	19	54	10	55	0
56	0	56	10	55	19	53	28	48	36	43	43	36	48	28	53	19	55	10	56	0
57	0	57	10	56	19	54	28	49	37	44	44	37	49	28	54	19	56	10	57	0
58	0	58	10	57	20	54	29	50	37	44	44	37	50	29	54	20	57	10	58	0
59	0	59	10	58	20	55	30	51	38	45	45	38	51	30	55	20	58	10	59	0
60	0	60	10	59	21	56	30	52	39	46	46	39	52	30	56	21	59	10	60	0

Wind speed

61	0	61	11	60	21	57	30	53	39	47	47	39	53	30	57	21	60	11	61	0
62	0	62	11	61	21	58	31	54	40	48	48	40	54	31	58	21	61	11	62	0
63	0	63	11	62	22	59	32	55	41	48	48	41	55	32	59	22	62	11	63	0
64	0	64	11	63	22	60	32	55	41	49	49	41	55	32	60	22	63	11	64	0
65	0	65	11	64	22	61	32	56	42	50	50	42	56	32	61	22	64	11	65	0
66	0	66	11	65	23	62	33	57	42	51	51	42	57	33	62	23	65	11	66	0
67	0	67	12	66	23	63	34	58	43	51	51	43	58	34	63	23	66	12	67	0
68	0	68	12	67	23	64	34	59	44	52	52	44	59	34	64	23	67	12	68	0
69	0	69	12	68	24	65	34	60	44	53	53	44	60	34	65	24	68	12	69	0
70	0	70	12	69	24	66	35	61	45	54	54	45	61	35	66	24	69	12	70	0
71	0	71	12	70	24	67	36	62	46	54	54	46	62	36	67	24	70	12	71	0
72	0	72	13	71	25	68	36	62	46	55	55	46	62	36	68	25	71	13	72	0
73	0	73	13	72	25	69	36	63	47	56	56	47	63	36	69	25	72	13	73	0
74	0	74	13	73	25	70	37	64	48	57	57	48	64	37	70	25	73	13	74	0
75	0	75	13	74	26	70	38	65	48	57	57	48	65	38	70	26	74	13	75	0
76	0	76	13	75	26	71	38	66	49	58	58	49	66	38	71	26	75	13	76	0
77	0	77	13	76	26	72	38	67	50	59	59	50	67	38	72	26	76	13	77	0
78	0	78	14	77	27	73	39	68	50	60	60	50	68	39	73	27	77	14	78	0
79	0	79	14	78	27	74	40	68	51	61	61	51	68	40	74	27	78	14	79	0
80	0	80	14	79	27	75	40	69	51	61	61	51	69	40	75	27	79	14	80	0
81	0	81	14	80	28	76	40	70	52	62	62	52	70	40	76	28	80	14	81	0
82	0	82	14	81	28	77	41	71	53	63	63	53	71	41	77	28	81	14	82	0
83	0	83	14	82	28	78	42	72	53	64	64	53	72	42	78	28	82	14	83	0
84	0	84	15	83	29	79	42	73	54	64	64	54	73	42	79	29	83	15	84	0
85	0	85	15	84	29	80	42	74	55	65	65	55	74	42	80	29	84	15	85	0
86	0	86	15	85	29	81	43	74	55	66	66	55	74	43	81	29	85	15	86	0
87	0	87	15	86	30	82	44	75	56	67	67	56	75	44	82	30	86	15	87	0
88	0	88	15	87	30	83	44	76	57	67	67	57	76	44	83	30	87	15	88	0
89	0	89	15	88	30	84	44	77	57	68	68	57	77	44	84	30	88	15	89	0
90	0	90	16	89	31	85	45	78	58	69	69	58	78	45	85	31	89	16	90	0
91	0	91	16	90	31	85	46	79	59	70	70	59	79	46	85	31	90	16	91	0
92	0	92	16	91	31	86	46	80	59	70	70	59	80	46	86	31	91	16	92	0
93	0	93	16	92	32	87	46	81	60	71	71	60	81	46	87	32	92	16	93	0
94	0	94	16	93	32	88	47	81	60	72	72	60	81	47	88	32	93	16	94	0
95	0	95	16	94	32	89	48	82	61	73	73	61	82	48	89	32	94	16	95	0
96	0	96	17	95	33	90	48	83	62	74	74	62	83	48	90	33	95	17	96	0
97	0	97	17	96	33	91	48	84	62	74	74	62	84	48	91	33	96	17	97	0
98	0	98	17	97	34	92	49	85	63	75	75	63	85	49	92	34	97	17	98	0
99	0	99	17	98	34	93	50	86	64	76	76	64	86	50	93	34	98	17	99	0
100	0	100	17	98	34	94	50	87	64	77	77	64	87	50	94	34	98	17	100	0
101	0	101	18	99	35	95	50	87	65	77	77	65	87	50	95	35	99	18	101	0
102	0	102	18	100	35	96	51	88	66	78	78	66	88	51	96	35	100	18	102	0
103	0	103	18	101	35	97	52	89	66	79	79	66	89	52	97	35	101	18	103	0
104	0	104	18	102	36	98	52	90	67	80	80	67	90	52	98	36	102	18	104	0
105	0	105	18	103	36	99	52	91	68	80	80	68	91	52	99	36	103	18	105	0
106	0	106	18	104	36	100	53	92	68	81	81	68	92	53	100	36	104	18	106	0
107	0	107	19	105	37	101	54	93	69	82	82	69	93	54	101	37	105	19	107	0
108	0	108	19	106	37	102	54	94	69	83	83	69	94	54	102	37	106	19	108	0
109	0	109	19	107	37	102	54	94	70	84	84	70	94	54	102	37	107	19	109	0
110	0	110	19	108	38	103	55	95	71	84	84	71	95	55	103	38	108	19	110	0
111	0	111	19	109	38	104	56	96	71	85	85	71	96	56	104	38	109	19	111	0
112	0	112	19	110	38	105	56	97	72	86	86	72	97	56	105	38	110	19	112	0
113	0	113	20	111	39	106	56	98	73	87	87	73	98	56	106	39	111	20	113	0
114	0	114	20	112	39	107	57	99	73	87	87	73	99	57	107	39	112	20	114	0
115	0	115	20	113	39	108	58	100	74	88	88	74	100	58	108	39	113	20	115	0
116	0	116	20	114	40	109	58	100	75	89	89	75	100	58	109	40	114	20	116	0
117	0	117	20	115	40	110	58	101	75	90	90	75	101	58	110	40	115	20	117	0
118	0	118	20	116	40	111	59	102	76	90	90	76	102	59	111	40	116	20	118	0
119	0	119	21	117	41	112	60	103	77	91	91	77	103	60	112	41	117	21	119	0
120	0	120	21	118	41	113	60	104	77	92	92	77	104	60	113	41	118	21	120	0

TABLE A-II

Wind Resolution to X (west-east) and Y (south-north) Components

(W_x, W_y)

Wind direction	Wind speed 1-9		10-19		20-29		30-39		40-49		50-59		60-74		75-99		100-149	
N	0	-4.5	0	-14.5	0	-24.5	0	-34.5	0	-44.5	0	-54.5	0	-67.0	0	-87.0	0	-124.5
NNE	-1.7	-4.2	-5.5	-13.4	-9.4	-22.7	-13.2	-31.9	-17.0	-41.1	-20.9	-50.4	-25.6	-61.9	-33.3	-61.9	-47.6	-115.0
NE	-3.2	-3.2	-10.2	-10.2	-17.3	-17.3	-24.4	-24.4	-31.5	-31.5	-38.5	-31.5	-47.4	-47.4	-61.5	-61.5	-88.0	-88.0
ENE	-4.2	-1.7	-13.4	-5.5	-22.7	-9.4	-31.9	-13.2	-41.1	-17.0	-50.4	-20.9	-61.9	-25.6	-80.4	-33.3	-115.0	-47.6
E	-4.5	0	-14.5	0	-24.5	0	-34.5	0	-44.5	0	-54.5	0	-67.0	0	-87.0	0	-124.5	0
ESE	-4.2	1.7	-13.4	5.5	-22.7	+9.4	-31.9	13.2	-41.1	17.0	-50.4	20.9	-61.9	25.6	-80.4	33.3	-115.0	47.6
SE	-3.2	3.2	-10.2	10.2	-17.3	17.3	-24.4	24.4	-31.5	31.5	-38.5	38.5	-47.4	47.4	-61.5	61.5	-88.0	88.0
SSE	-1.7	4.2	-5.5	13.4	-9.4	22.7	-13.2	31.9	-17.0	41.1	-20.9	50.4	-25.6	61.9	-33.3	80.4	-47.6	115.0
S	0	+4.5	0	+14.5	0	+24.5	0	+34.5	0	44.5	0	54.5	0	67.0	0	87.0	0	124.5
SSW	1.7	4.2	+5.5	13.4	9.4	22.7	13.2	31.9	17.0	41.1	20.9	50.4	25.6	61.9	33.3	80.4	47.6	115.0
SW	3.2	3.2	10.2	10.2	17.3	17.3	24.4	24.4	31.5	31.5	38.5	38.5	47.4	47.4	61.5	61.5	88.0	88.0
WSW	4.2	1.7	13.4	5.5	22.7	9.4	31.9	13.2	41.1	17.0	50.4	20.9	61.9	25.6	80.4	33.3	115.0	47.6
W	4.5	0	14.5	0	24.5	0	34.5	0	44.5	0	54.5	0	67.0	0	87.0	0	124.5	0
WNW	4.2	-1.7	13.4	-5.5	22.7	-9.4	31.9	-13.2	41.1	-17.0	50.4	-20.9	61.9	-25.6	80.4	-33.3	115.0	-47.6
NW	3.2	-3.2	10.2	-10.2	17.3	-17.3	24.4	-24.4	31.5	-31.5	38.5	-38.5	47.4	-47.4	61.5	-61.5	88.0	-88.0
NNW	1.7	-4.2	5.5	-13.4	9.4	-22.7	13.2	-31.9	17.0	-41.1	20.9	-50.4	25.6	-61.9	33.3	-80.4	47.6	-115.0

TABLE A-III

Component Squares

(W_x^2, W_y^2)

Wind direction	Wind speed 1-9		10-19		20-29		30-39		40-49		50-59		60-74		75-99		100-149	
N	0	20	0	210	0	600	0	1190	0	1980	0	2970	0	4489	0	7569	0	15500
NNE	3	18	30	180	88	515	174	1018	289	1687	437	2540	655	3832	1109	6464	2266	13225
NE	10	10	104	104	299	299	595	595	992	992	1482	1482	2247	2247	3782	3782	7744	7744
ENE	18	3	180	30	515	88	1018	174	1689	289	2540	437	3832	655	6464	1109	13225	2266
E	20	0	210	0	600	0	1190	0	1980	0	2970	0	4489	0	7569	0	15500	0
ESE	18	3	180	30	515	88	1018	174	1689	289	2540	437	3832	655	6464	1109	13225	2266
SE	10	10	104	104	299	299	595	595	992	992	1482	1482	2247	2247	3782	3782	7744	7744
SSE	3	18	30	180	88	515	174	1018	289	1689	437	2540	655	3832	1109	6464	7266	13225
S	0	20	0	210	0	600	0	1190	0	1980	0	2970	0	4489	0	7569	0	15500
SSW	3	18	30	180	88	515	174	1018	289	1689	437	2540	655	3832	1109	6464	2266	13225
SW	10	10	104	104	299	299	595	595	992	992	1482	1482	2247	2247	3782	3782	7744	7744
WSW	18	3	180	30	515	88	1018	174	1689	289	2540	437	3832	655	6464	1109	13225	2266
W	20	0	210	0	600	0	1190	0	1980	0	2970	0	4489	0	7569	0	15500	0
WNW	18	3	180	30	515	88	1018	174	1689	289	2540	437	3832	655	6464	1109	13225	2266
NW	10	10	104	104	299	299	595	595	992	992	1482	1482	2247	2247	3782	3782	7744	7744
NNW	3	18	30	180	88	515	174	1018	289	1689	437	2540	655	3832	1109	6464	2266	13225

TABLE A-IV

Covariances

(W_x, W_y)

Wind direction	Wind speed 1-9	10-19	20-29	30-39	40-49	50-59	60-74	75-99	100-149
N	0	0	0	0	0	0	0	0	0
NNE	7	74	213	421	699	1053	1585	2677	5474
NE	10	104	299	595	992	1482	2247	3782	7744
ENE	7	74	213	421	699	1053	1585	2677	5474
E	0	0	0	0	0	0	0	0	0
ESE	-7	-74	-213	-421	-699	-1053	-1585	-2677	-5474
SE	-10	-104	-299	-595	-992	-1482	-2247	-3782	-7744
SSE	-7	-74	-213	-421	-699	-1053	-1585	-2677	-5474
S	0	0	0	0	0	0	0	0	0
SSW	7	74	213	421	699	1053	1585	2677	5474
SW	10	104	299	595	992	1482	2247	3782	7744
WSW	7	74	213	421	699	1053	1585	2677	5474
W	0	0	0	0	0	0	0	0	0
WNW	-7	-74	-213	-421	-699	-1053	-1585	-2677	-5474
NW	-10	-104	-299	-595	-992	-1482	-2247	-3782	-7744
NNW	-7	-74	-213	-421	-699	-1053	-1585	-2677	-5474

LIST OF REFERENCES

1. Reed, J. W., Estimating Safety Probabilities from Fallout Forecasts at Nevada Test Site, SC-4073(TR), February 1957.

2. Reed, J. W., "The Representativeness of Winds Aloft Observations," Bulletin of the American Meteorological Society, Vol. 35, No. 6, June 1954.

3. Singer, B. M., "Wind Variability as a Function of Time at Muroc, California," Bulletin of the American Meteorological Society, Vol. 37, No. 5, May 1956.

4. Reed, J. W. and VanZandt, T. E., Wind and Position Variability from Rawijet Data, SC TM-61-57-51, February 1957.

5. Tables of Winds and Their Aiding and Retarding Effect at 850, 700, 500, 300, and 200 mb, Part 3, U.S., NAVAER 50-1C-526, Washington.

6. Crutcher, H. L., "On the Standard Vector Deviation Wind Rose," Journal of Meteorology, Vol. 14, No. 1, February 1957.

7. Arnold, A., Representative Winds Aloft, BAMS Vol. 37, No. 1, January 1956.

8. "The Variation of Wind with Distance; the Variation of Wind with Time," Meteorological Office Memoir No. 389, Air Ministry Meteorological Office, London.

9. Plagge, H. J. and Smith, L. B., Project Rawijet--A Study of the Wind Variability in Space and Time at the Salton Sea Test Base, SC-3880(TR), December 10, 1956.

10. Bryson, R. A., The Time-Variation of Certain Large-Scale Circulation Parameters, paper presented to the American Meteorological Society, Asheville, North Carolina, October 29, 1956.

11. Reeves, J. E., Test Manager's Standard Operating Procedure for the Nevada Test Organization, ETP: MFS-3621, AEC Albuquerque Operations Office, March 15, 1957.

12. Buell, C. E. and Stoddard, D. W., CLASSIFIED TITLE, Sandia Corporation TM-289-56-51, January 11, 1957, SECRET (Referenced information declassified and to be published in open literature).

13. Mastenbrook, H. J., Transosonde Flights for 1955, Naval Research Laboratory Memorandum Report 612, June 1956.

14. Owen, D. B., The Bivariate Normal Probability Distribution, SC-3831(TR), August 1, 1956.

15. Reed, J. W., Objective Adjustment of NPG Winds Aloft Forecasts, SC TM-128-54-51, June 25, 1954.

16. Reed, J. W., Some Additional Notes on Winds Aloft Forecasting for NPG, SC TM-155-54-51, August 17, 1954.

INITIAL DISTRIBUTION:

1	Jean O'Leary, DMA
2-4	K. F. Hertford, ALO Attn: J. E. Reeves R. H. Goeke
5	A. E. Uehlinger, ALO, Sandia
6-10	Helen Redman, LASL Attn: N. E. Bradbury A. C. Graves W. E. Ogle W. R. Kennedy O. W. Stopinski
11-13	Margaret Edlund, UCRL Attn: D. Sewell G. W. Johnson A. V. Shelton
14	K. H. Larsen, UCLA
15	E. Schuert, NRDL
16	G. M. Dunning, AEC/DBM
17	P. W. Allen, USWB, AEC/LVBO
18	L. Machta, USWB, Washington, D. C.
19	R. L. Corsbie, Civil Defense Liaison Branch, AEC/DBM
20	W. W. Kellogg, RAND Corporation
21	O. Placek, USPHS, AEC/LVBO
22-126	AFSWP 22-119 Standard AFSWP distribution 120 Col. K. D. Coleman, FC 121 J. L. Magee, OSD/WSEG 122 R. Willis, APG, BRL 123 Cdr. D. F. Rex, JTF-7 (Meteorological Center, Pearl Harbor) 124 Lt. Col. V. L. Boling, USA A&M School, Ft. Sill, Oklahoma 125 Lt. Col. A. R. Gill, OSWD, Ft. Bliss, Texas 126 D. M. Swingle, SCEL, Ft. Monmouth, New Jersey
127-160	AFSWC 127-158 Standard AFSWC distribution 159 Col. J. J. Jones, AWS, 4th Group, Baltimore 160 W. L. Molo, AWS, D Clim, Andrews AFB, Washington
161	G. A. Fowler, 5000
162	S. C. Hight, 5100
163	R. A. Bice, 5200
164	M. L. Merritt, 5110
165	D. B. Shuster, 5230
166	T. B. Cook, 5111
167	J. W. Reed, 5111
168	B. N. Charles, 5122
169	H. J. Plagge, 5243
170	A. E. Jones, 2464
171-180	Document Room

B DISTRIBUTION:

181-505	TISE
506-605	OTS
606-615	W. K. Cox, 3466-1